International Society for Biofabrication
PURPOSE-LED PUBLISHING™

TOPICAL REVIEW • **OPEN ACCESS**

Engineering breast cancer tumor microenvironment: advanced fabrication for 3D *in vitro* models

To cite this article: M Pitton *et al* 2026 *Biofabrication* **18** 012006

View the article online for updates and enhancements.

You may also like

- Recapitulating the human myotendinous junction *in vitro* using a 3D bioprinted model
Francesca De Paolis, Marina Volpi, Claudia Fuoco et al.
- A mechanically active nucleus pulposus-on-a-chip for studying mechanobiology and therapeutic strategies in intervertebral disc disease
Olga Krupkova, Bianca Aterini, Nader Rahal et al.
- Self-driving bioprinting laboratories
Suihong Liu, Navneet Kaur, Dae-Hyeon Song et al.

This content was downloaded from IP address 131.175.66.152 on 09/03/2026 at 07:08

Biofabrication

Check for updates

TOPICAL REVIEW

Engineering breast cancer tumor microenvironment: advanced fabrication for 3D *in vitro* models

M Pitton[1], L Draghi[1,2] and S Farè[1,2,*]

[1] Department of Chemistry, Materials and Chemical Engineering 'G. Natta', Politecnico di Milano, Milan, Italy
[2] INSTM Local Unit, Politecnico di Milano, Milan, Italy
[*] Author to whom any correspondence should be addressed.

E-mail: silvia.fare@polimi.it

Keywords: spheroids, organ-on-chips, scaffolds, hydrogels, bioprinting

OPEN ACCESS

RECEIVED
1 June 2025

REVISED
23 October 2025

ACCEPTED FOR PUBLICATION
16 January 2026

PUBLISHED
5 February 2026

Original content from this work may be used under the terms of the Creative Commons Attribution 4.0 licence.

Any further distribution of this work must maintain attribution to the author(s) and the title of the work, journal citation and DOI.

Abstract

The investigation of breast cancer initiation and progression has been significantly advanced by the development of three-dimensional (3D) in vitro models, which provide a more physiologically relevant representation of the tumor microenvironment (TME) compared to conventional two-dimensional cultures. Over the past decade, and particularly since 2020, a wide range of strategies has been developed to generate stable and functional 3D breast cancer models. This review provides a comprehensive overview of the most promising (bio)fabrication-based technologies developed for breast cancer modeling, critically discussing their applications, advantages, limitations, and future perspectives. Among current approaches, tumor spheroids have demonstrated considerable value due to their characteristic architecture, comprising a necrotic core surrounded by proliferative and quiescent cell layers, which partially mimics in vivo tumor organization. In parallel, organ-on-chip (OoC) systems have emerged as powerful platforms for drug screening and therapeutic testing, enabling dynamic culture conditions within microengineered and perfusable environments. However, spheroids lack an external extracellular matrix, while the compartmentalized nature of OoCs systems limits their ability to fully reproduce the structural and compositional complexity of the breast TME. To address these limitations, engineered 3D-printed scaffolds and constructs produced through biofabrication approaches have gained increasing attention. In particular, natural hydrogel-based systems offer high biocompatibility and tunable biochemical and mechanical properties, enabling the co-culture of malignant and healthy cells and supporting more predictive evaluations of anticancer therapies.

1. Introduction

Breast cancer remains the most frequently diagnosed malignancy in women all over the world, and the primary cause of cancer-related mortality. The Global Cancer Observatory (GLOBOCAN), from the International Agency for Research on Cancer, has reported that 19.3 million new cancer cases and 10.0 million cancer related deaths occurred in 2020 [1]. Among these, breast cancer accounted for 2.26 million cases in 2020, followed by lungs (2.21 million cases) and prostate (1.41 million cases) cancers. Despite advances in early detection and the introduction of novel screening tools that have reduced overall mortality, breast cancer still represents the prominent cause of death in females. Additionally, GLOBOCAN projections depict a dramatic scenario in the next years, predicting breast cancer incidence to grow disproportionately in countries with a relatively low Human Development Index (referred to economic development), e.g. Middle and Eastern Africa, South-Central Asia and Melanesia [2]. Globally, new cases are expected to rise from 2261 419 in 2020 to 3025 471 in 2040; moreover, associated deaths are estimated to increase from 684 996 in 2020 to 1037 723 in 2040 [1].

For decades, two-dimensional (2D) cell cultures have served as the standard *in vitro* approach to model breast cancer cells growth and drugs resistance. These 2D systems routinely use established cell lines or cells extracted from patient-derived xenografts to investigate tumor biology and novel therapeutic strategies

© 2026 The Author(s). Published by IOP Publishing Ltd

against breast cancer [3]. However, 2D approaches fail to replicate the complexity of tumorigenesis. They do not capture the interaction between cancerous and non-cancerous cells, the influence of the extracellular matrix (ECM) on intracellular pathways, nor the presence of soluble factors [4, 5]. Alternatively, genetically engineered mouse models have been frequently used to study breast cancer initiation, development, and metastatic progression in living and dynamic tissues, enabling the investigation of proto-oncogenes expression or tumor suppressors deletion [6–8]. However, animal models are costly, labor-intensive, time-consuming, and ethically controversial. Additionally, they do not offer clear insights on human response to drug treatments, limiting their translation relevance, a main objective in oncology research [9].

To address these limitations, drug testing platforms capable of bridging the gap between 2D cultures and animal models are needed. Recently, 3D *in vitro* models have emerged as reliable solutions to study the complex and intricate mechanisms behind breast cancer origin and progression, demonstrating good correlation with *in vivo* outcomes. The main advantage of 3D *in vitro* models resides in their ability to sustain cell viability, proliferation, and communication in a more relevant microenvironment [10]. This enlightens the complex crosstalk between tumor cells and other cell types (e.g. non-cancer stromal cells, endothelial cells, inflammatory cells, adipocytes, and immune cells), or between tumor cells and the outer space, thereby revealing new potential therapeutic targets [11].

1.1. The breast tumor microenvironment (TME)

The contribution of the surrounding breast microenvironment in tumorigenesis is now well established [12, 13]. We define breast TME as an altered and chaotic matrix composed of various infiltrating immune cells, e.g. tumor-associated macrophages, lymphocytes, and other stromal cells, and ECM, which together participate in cell–cell and cell-matrix interactions, orchestrating the breast tumor progression [14]. Interestingly, the recent growth of oncology research interest in the contribution of the TME in breast tumorigenesis is also well reflected in publication trends. PubMed publications on the *Breast TME role* rapidly increased from 2017 (100) to 2023 (248) However, despite the recognized role of TME, unveiling the precise mechanisms of cellular communication within the TME and its concrete contribution in tumorigenesis is still challenging, since matrix composition and features completely mutate during the progression of breast cancer.

In pathological conditions, a cascade of mechanisms can occur in breast tissues, progressively establishing the TME (figure 1). Fatty acid production by mature adipocytes is dramatically reduced due to the low expression of receptor ERα36. Additionally, hypoxia inducing factors (HIFs) are overexpressed by cancer cells, which consequently establish a condition of oxygen deprivation in TME. Hypoxia promotes cancer progression by altering metabolic pathways, and trigger self-growth through glycogen metabolism reprogramming as the glycogen program pathway decreases the number of circulating immune cells, increasing the mortality rate. Furthermore, hypoxia induces chemoresistance in breast cancer cells, as well as the formation of areas of necrotic cells, and it also stimulates neo-angiogenesis processes, enabling cancer cell migration and metastatic dissemination. ECM remodeling occurs through the accumulation of hyaluronic acid (HA) between the proliferating cancer cells, and dense deposition of collagen (type I, III, V, VI), leading to matrix stiffening. Finally, downregulation of E-cadherin expression causes the loss of adhesion between myoepithelial and luminal cells in breast tissues [15–17].

Interactions between cancerous and non-cancerous cells are likewise pivotal for malignancy progression and remain poorly elucidated. In ductal carcinoma *in situ*, breast ductal epithelial cells form a central lumen, and cancerous cells arise from the healthy epithelium and proliferate into this lumen [18], forming a necrotic inner core, which is denser than the surrounding matrix. Consequently, malignant cells break through the basement membrane and acquire metastatic potential.

Another hallmark of breast TME is the pronounced metastatic propensity of breast cancer cells to move toward other anatomical districts, such as bone, lungs, liver, or brain [19]. Several deaths attributed to breast cancer have been strictly connected to metastasis processes [15]. Metastasis is a complex pathophysiological process that depends on the interplays between components of the TME and cancer cells. Mimicking metastasis in 2D cultures results challenging, while 3D models have proven highly valuable for evaluating breast cancer invasiveness and metastatic behavior [20, 21].

Accordingly, in the last decades, 3D *in vitro* models have gained interest in oncology research offering innovative and reliable platforms to reconstruct the TME and implement novel therapeutic strategies against breast cancer. These models can incorporate many additional aspects of the breast TME, including heterogeneous cell types, altered ECM composition and features, as well as growth factors and cytokine gradients [22].

1.2. Fabrication technologies for 3D models

3D *in vitro* models can be classified into two main categories based on their fabrication strategy [23]: scaffold-free cell aggregates cultures and fabricated scaffolds. In scaffold-free approaches cells are led to spontaneously aggregate in spheroidal and compact morphologies, without adhesion to external substrates. In contrast, scaffold-based techniques employ

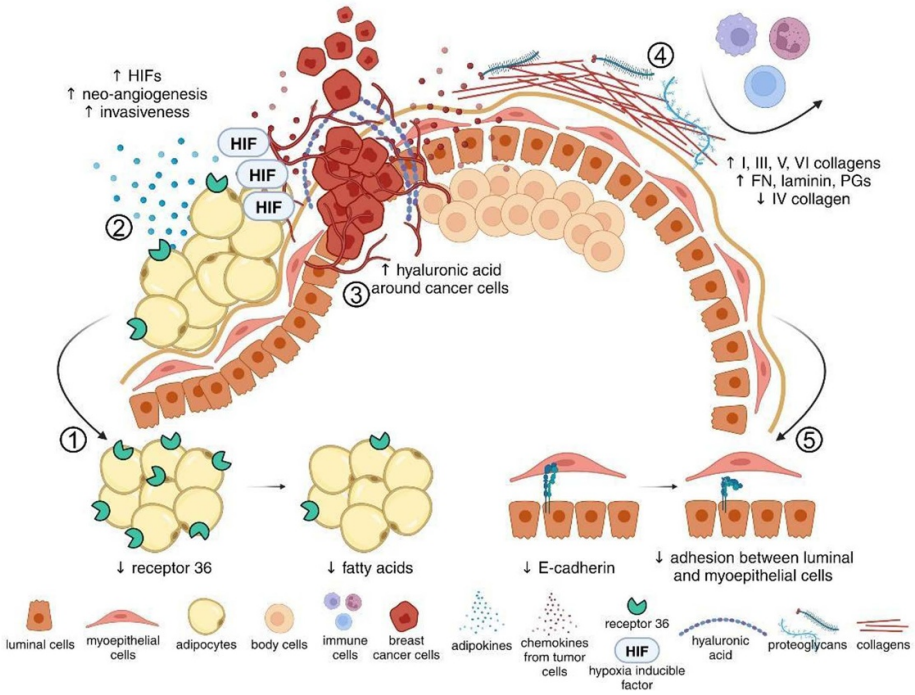

Figure 1. Breast TME. During tumorigenesis, different mechanisms have been recognized, by starting from adipocytes alterations in fatty acids uptake (1), consequent induction of neo-angiogenesis and invasiveness (2) due to HIFs release. Progressive proliferation of breast cancer cells from basal membrane increases the release of tumoral chemokines which promote ECM alterations (3)–(4) preventing from immune cells infiltration. Invasiveness of breast cancer cells into intralobular and interlobular stroma is favored by detachment of epithelial cells from basal membrane due to E-cadherin loss (5). Created in BioRender. Pitton (2026) https://BioRender.com/a1l6cil.

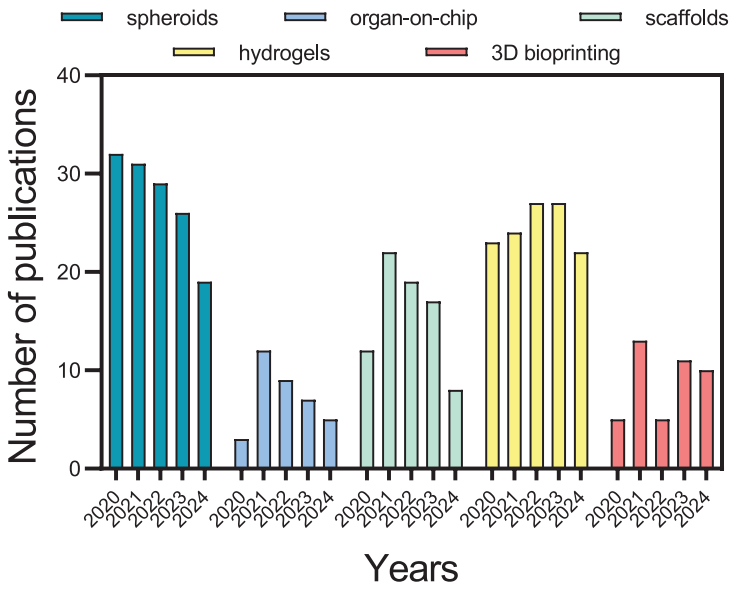

Figure 2. Number of publications (per year) on fabrication approaches involved in 3D *in vitro* models' development for breast TME mimicking (from 2020 up to 2024). *Data source: Pubmed.*

a 3D substrate where breast cancer cells can adhere and grow in engineered matrices, and drug effectiveness on such cells can be tested.

The urgent need for breast cancer investigation has stimulated the rapid development of 3D *in vitro* models with advanced fabrication technologies. Here, we focused on the articles published after 2020, to provide a detailed overview of how technological refinement has enabled the obtainment of evolved 3D *in vitro* breast cancer models (figure 2).

Given the tremendous interest gained by the role of TME in breast cancer origin and development, complex functional models comprising structural organization with bioactive molecules, living cells,

and (sometimes) biomaterials have been developed. The main fabrication approaches for breast cancer modeling can be grouped in spheroid models, organ-on-chip models (OoC), and engineered 3D constructs, such as scaffold-based models, hydrogels, and bioprinted models. Publication trends enlighten how spheroid models have been the most widely employed technology to build 3D *in vitro* models for breast cancer for many years. The number of publications for spheroid models has doubled from 2017 (15) to 2020 (32), whereas it has remained approximately constant between 2020 and 2022 (29), with a subsequent decrease from 2022 up to 2024 (19) (*Pubmed, 2025; keywords: spheroids for breast cancer*). The use of spheroids replaced the use of simplistic 2D cell cultures especially for drug testing, but their use has been limited by the drawbacks in scalability and reproducibility [16]. A similar trend is observed for OoCs, whose publications significantly increased between 2017 (1) and 2021 (12), and then decreased up to 2024 (5) (*Pubmed, 2025; keywords: OoC for breast cancer*). The lower adoption rate of OoCs is probably due to the more complex and expensive technologies involved in OoCs fabrication [16].

In contrast, engineered 3D constructs (scaffold-based models, hydrogels, bioprinted models) have gained terrific interest. This rise parallels the increasing focus on breast TME and its role in pathology occurrence, as models enabled the integration of a relevant bioactive matrix surrounding breast cancer cells. Among 3D models, hydrogels and bioprinted models have surpassed traditional porous scaffolds (from 19 publications in 2019 to 8 papers in 2024; *Pubmed, 2025; keywords: 3D scaffolds for breast cancer*) [9]. Both hydrogels and bioprinted models enable direct embedding of living cells into polymeric and hydrophilic networks, fabricated via casting and molding (hydrogels) or scalable bioprinting (bioprinted models). In particular, interest in hydrogel-based models has steadily grown (from 14 publications in 2017 to 22 papers in 2024; *Pubmed, 2025; keywords: hydrogels for breast cancer*), probably thanks to their versatility and their tunable mechanical and biological properties, Conversely, bioprinted models have emerged more recently as a cutting-edge and versatile strategy, (raising from 2 publications in 2017 to 10 papers in 2024; *Pubmed, 2025; keywords: bioprinting for breast cancer*).

While several high-quality reviews on 3D breast cancer models have been already published [9, 16]. This field is rapidly evolving and demands continuous updates. Additionally, researchers have lately focused on specific applications related to breast cancer 3D modeling, e.g. endocrine therapy [24], radiobiology [25], nanomedicine [26], or on peculiar pathological, e.g. cancer metastasis [27–29], ductal carcinoma [30], or technological aspects, e.g. 3D printing [31].

On the other hand, aligning technological innovation with emerging clinical demands could accelerate the development of new approaches for personalized medicine and support their clinical translation. For this reason, we aim to provide a comprehensive and up-to-date overview of the main fabrication approaches for breast cancer 3D modeling, outlining their respective advantages and current limitations. For each investigated method, we focused on recent publications (2020–2024), and we detailed the used biomaterials (where applicable), cell types involved, the final application, and the main expected/obtained results. Ultimately, this review seeks to elucidate how technologies have evolved and accommodated the urgent requests from oncology research, and which techniques represent the most promising to bridge the gap between the past and the next-generation technologies.

2. Breast TME 3D *in vitro* models

2.1. Spheroids or mammospheres

Spheroids are micro-scale 3D *in vitro* models formed by densely packed cells aggregates ranging from 100 to 600 μm in diameter. These aggregates can form by self-assembling or forcibly induced to clusters. Specifically, the term *mammosphere* refers to those packed spheroids constituted by aggregated breast cancer cell lines [16]. As such, mammospheres have been extensively employed to investigate multiple aspects in breast cancer biology, including growth, proliferation, metabolism, and angiogenesis [11]. These spheroids have gained attention for TME mimicking for multiple relevant features [32–35]: critical size (μm dimensions); internal oxygen/nutrients/pH gradients, caused by impaired diffusion of molecules; heterogeneous interface with culture medium; prevalent cell junctions; increased volume growth kinetic; increased cell survival for a defined period of culture; high levels of stromal proteins and molecules secretion.

Spheroids typically exhibit three defined cell layers (figure 3) analogous to those found in avascular or poorly vascularized tumor nodules, micrometastasis, or intravascular regions of large solid tumors [5, 32]: an outer *proliferative* layer, which represents the proliferating area; an intermediate *zone of quiescent cells*; an inner *necrotic* area (or *core*), which spontaneously forms due to the lack of oxygen/nutrients/metabolites [36].

The presence of an inner necrotic portion is a hallmark of mammospheres and makes spheroids to be widely considered for antitumor drug screening tests. Central necrosis and diffusion limitations may impact drug penetration and modeling drug penetration in solid tumors results more accurate than in 2D systems [33, 37]. At the same time, oxygen/nutrients exchanges are more prominent in external layers, and breast cancer cells can migrate from the inner core

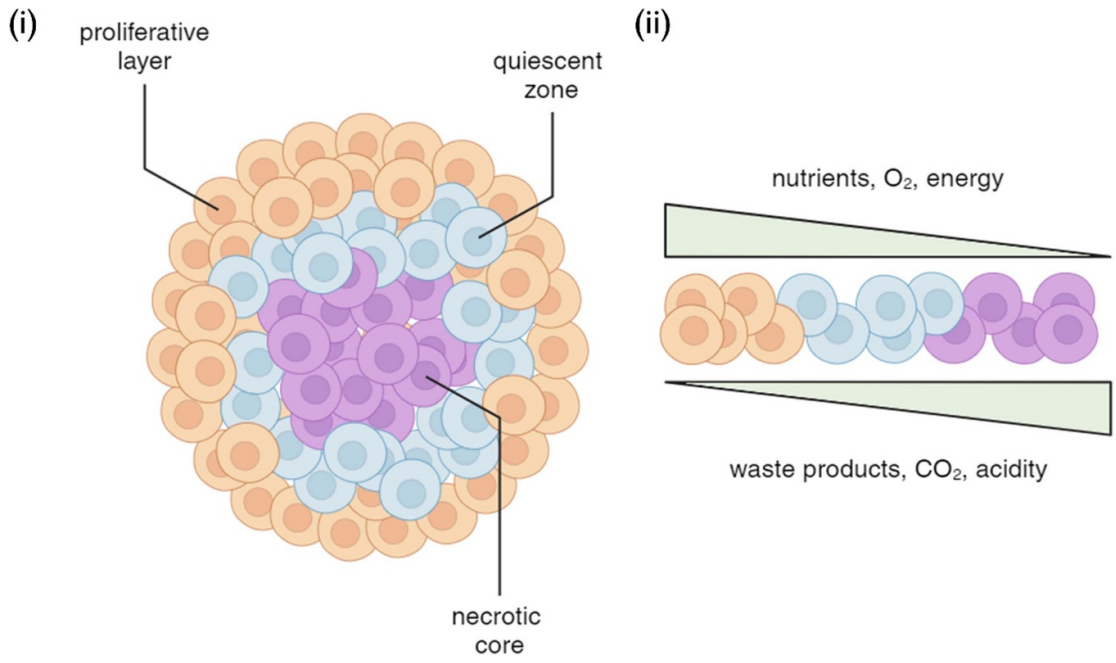

Figure 3. In spheroids, three main portions can be distinguished: an external proliferative layer, an intermediate quiescent zone, and an inner necrotic core (i). By considering different portions of the spheroids, cells can receive more nutrients, oxygen and energy (in form of ATP) (from outer to inner zone), or can exchange more waste products, carbon dioxide and acidity (from inner to outer zone) (ii). Created in BioRender. Pitton (2026) https://BioRender.com/jmk9tbm.

to superficial layers; this trivial feature consequently has been exploited for cells migration and invasion studies.

Spheroids dimensions deeply influence the biological functions of aggregated cells due to the establishment of internal diffusion gradients for oxygen, nutrients, and biochemical messengers. Smaller spheroids (100–300 μm) do not exhibit gradient-related variations in cell survival, thus providing a more homogeneous environment to investigate cell–cell and cell-TME interactions, expression profiles, and proliferation rate with greater fidelity than 2D cultures. Contrarily, larger spheroids (400–600 μm) are particularly valuable for investigating hypoxia, due to the presence of the necrotic internal core (100–300 μm) and a thick outer shell. Medium size spheroids (300–400 μm) show biochemical gradients at different portions, as periphery cells constitute an active proliferative layer, whereas most inward are quiescent or hypoxic; their core allows to mimic the pre-metastatic form of breast cancer or avascular tumors [36]. For these reasons, the size of the spheroids represents a major critical aspect and defining an ideal range of dimensions (in μm) is still a challenge. Prior studies have shown how small spheroids tend to lose oxygen, nutrients, and biochemical compound gradients, whereas large spheroids comprise an extensive necrotic core, making their biological relevance questionable [16]. Therefore, medium sized spheroids (300–500 μm) are generally considered an optimal compromise between size, internal gradients, and biological features.

2.1.1. Technologies for spheroids formation

Different methods have been developed to generate mammospheres (figure 4): hanging drop method; spinner flasks or suspended cell cultures; liquid overlay technique; 3D printing; aqueous two-phase system; magnetic levitation. The advantages and disadvantages of these approaches are summarized in table 1.

The hanging drop method involves the suspension of tumor cells in drops of culture medium, manually dispensed on a plate (typically the lid of a culture plate), and cultured upside-down [9] (figure 4(A)) with gravity inducing aggregation and spheroid formation. The viscosity of culture medium can be increased by adding a viscous component, such as methylcellulose, to enhance cohesive forces between cells to form clusters [5]. Both gravitational and cohesive forces thus act together in the aggregation mechanisms of spheroids. Hanging drop method allows a more accurate control of the initial number of cells per spheroid compared to suspended cell cultures or aqueous two-phase systems, increasing the reproducibility of the process. Other advantages are related to its easy implementation and low costs. Limitations are associated with the need for a rigorous standardization process. Recent implementations, such as 3D printed hanging-drop dripper, with automated droplet dispensing have improved reproducibility, bypassing drawbacks of manual pipetting [23, 34]. However, evaporation of culture medium causes difficulties in long-term cell cultures, and refilling or exchanging cell culture medium without

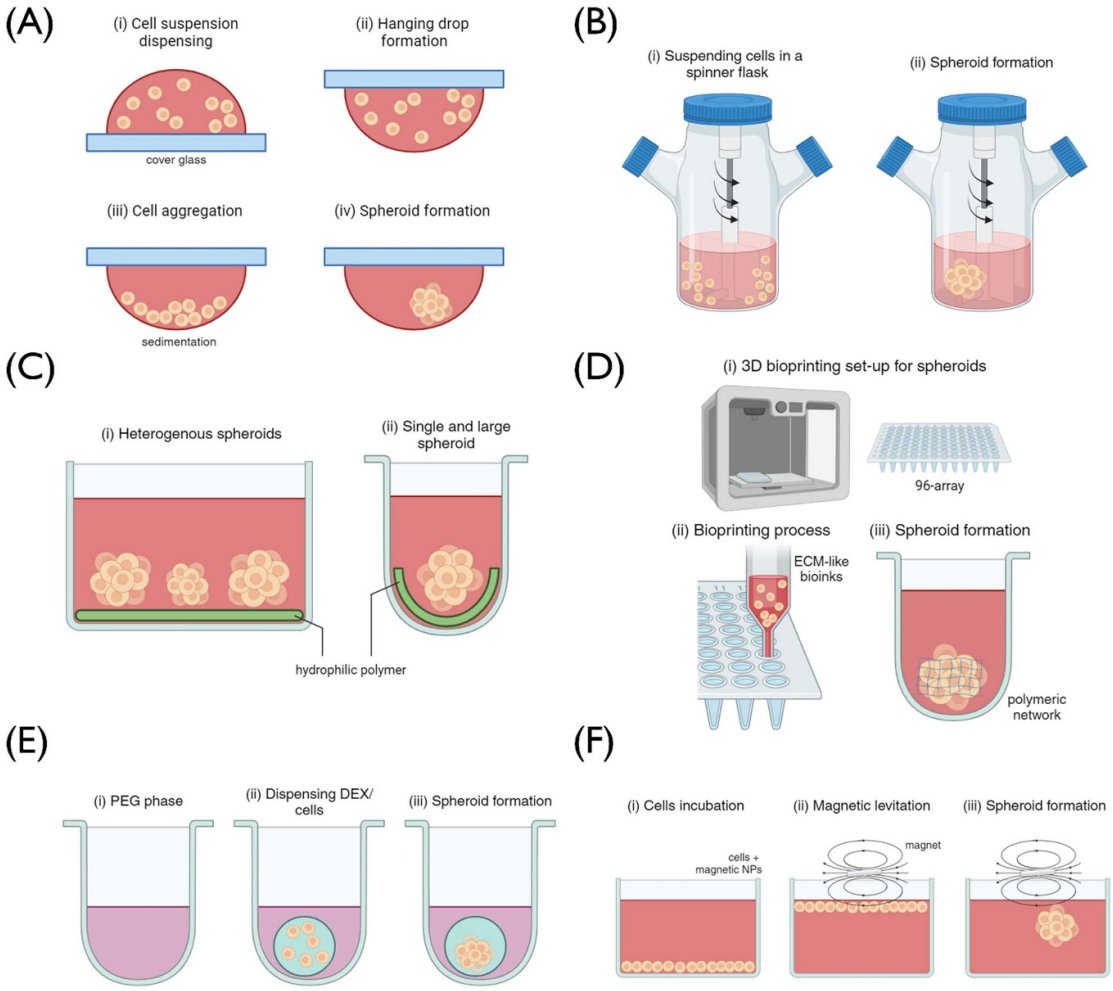

Figure 4. Technologies for spheroids formation. (A) Hanging drop. (B) Spinner flasks or suspended cell cultures. (C) Liquid overlay technique. (D) 3D Bioprinting. (E) Aqueous two-phase system. (F) Magnetic levitation technique. Created in BioRender. Pitton (2026) https://BioRender.com/ubhuu5o. Created in BioRender. Pitton (2026) https://BioRender.com/mi0cs89. Created in BioRender. Pitton (2026) https://BioRender.com/1ezlhq0 Created in BioRender. Pitton (2026) https://BioRender.com/ h516mx6. Created in BioRender. Pitton (2026) https://BioRender.com/jbtw75k. Created in BioRender. Pitton (2026) https://BioRender.com/v25z1d7.

compromising the droplets integrity result complicated. Other drawbacks can be associated with the difficulty of handling culture plates during the tests, and to the risks of transferring spheroids to a standard well plate.

Spinner flasks or suspended cell cultures consist of continuous spinning or stirring cells in spinner flasks. The continuous motion prevents cells from adhering to the flask surfaces and induces them to aggregate in spheroids [9, 41] (figure 4(B)). Treated or non-adhesive surfaces can be used [41]. Suspension cultures offer easy application, low costs, and possibility to scale-up; however, they suffer from lack of cells adhesion, size and shape variability, and to the need of specialized equipment [5, 34]. In addition, a rigorous standardization is required to avoid cell damage, potentially exposed to non-physiological shear forces, resulting in randomly sized spheroids that lack reproducibility.

Liquid overlay technique promotes cells aggregation in spheroids by culturing tumor cells in round-bottom well plates, pre-coated with non-adhesive polymers, as agarose or polyethylene glycol (PEG) [16] (figure 4(C)). Liquid overlay technique allows to obtain uniformly sized mammospheres, tipically one per well, and facilitates co-cultures. Tumor cells cultured with stromal fibroblasts have been used to examine cellular communication during spheres growth, differentiation and invasion [11]. The main limitation of this approach lies in the need for proper parameters for cell cultures and to the acquisition of a sufficient skill level to obtain regular sized spheroids.

3D bioprinting is a more recent and highly reproducible approach for developing mammospheres leveraging additive manufacturing (AM) technologies (figure 4(D)). It ensures the incorporation of living cells in biomaterials extruded intermittently as small droplets [22], providing a strict control over cells distribution and spheroids size, and over spatial placement of aggregates [9, 34, 38]. Improvements in AM have consequently increased flexibility, precision, and applicability of spheroid formation process.

Table 1. Advantages vs disadvantages of fabrication technologies for 3D spheroids.

	Advantages	Disadvantages	References
Hanging drop	↑ reproducibility ↓ costs Easy implementation	Rigorous standardization Culture medium evaporation	[23, 34]
Suspended cultures	↓ costs Easy application Scale-up production	↓ reproducibility Rigorous standardization Specialized equipment Non-physiological shear forces	[5, 34]
Liquid overlay	↑ reproducibility ↑ complexity	Rigorous standardization Difficult handling	[11, 16]
3D bioprinting	↑ reproducibility ↑ complexity and precision ↑ cell viability and cell-ECM adhesion	Difficult implementation Difficult handling Specialized equipment	[22, 36, 38, 39]
Aqueous two phase	↑ hydrophilic microenvironment ↑ diffusion and exchanges ↑ tumor biological features	↓ reproducibility	[9, 40]
Magnetic levitation	↑ reproducibility ↓ time in developing spheroids	Difficult implementation Difficult handling Specialized equipment	[9, 16]

Highly complex mammospheres can be obtained by bioprinting cell-laden materials. For example, breast cancer spheroids have been bioprinted by using different bioinks (Matrigel, gelatin-alginate, collagen-alginate) directly into an endothelial cells-laden structure made of collagen and alginate to study cell–cell interaction [22]. Recent technologies have improved 3D bioprinted spheroid obtainment, as the possibility to implement a pulsed laser which is able to deposit material from a printing ribbon to a receiving substrate [36]. These upgrades had a great impact on spatial resolution, and on the possibility to dispense viscous or small volumes with high precision. Still, the high costs, as well as the difficulties in its implementation and control, remain the main limitations.

Aqueous two-phase system utilizes two immiscible aqueous solutions to confine cells into the hydrophilic phase, resulting in drops formation and in the development of mammospheres [9] (figure 4(E)). The obtained spheroids are compact and show a standardized size. Breast tumor features have been investigated [40] for example, in spheroids obtained by mixing sub-microliter drops of a denser polymeric aqueous phase (PEG), containing cancer cells, in a dextran (DEX) aqueous phase. In the two-phase approach, diffusion of nutrients from the immersion phase to cells and removal of cells waste products from the drop phase are facilitated. Poor control of cell number and movement in the two aqueous phases, which can affect the reproducibility of the method, remain the main drawbacks.

Magnetic levitation technique promotes cells aggregation using magnetic nanoparticles incorporated into the cells and an external magnetic field [9, 16] (figure 4(F)). Magnetic levitation requires costly equipment and technical expertise [42], but enables rapid spheroid formation.

2.1.2. State-of-the-art spheroids and their evolution

Spheroids gained attention in cancer oncology due to their better performances in drug tests compared to 2D cell cultures [5, 9, 32, 33, 37]. Their main advantages are namely: higher degree of complexity, due to a more accurate mimicking of tumor biology; higher scalability to carry on investigations; lower associated costs; more cell–cell interactions; more similarities in architecture, oxygen/nutrients/cell proliferation gradients, and heterogeneity to tumors.

Mammospheres have been initially thought to investigate anticancer drugs penetration in the internal necrotic core and their effects over aggregated tumor cells (table 2). Chen *et al* fabricated MCF7 spheroids in low adhesion plates, and investigated the effects of different anticancer drugs, aiming to the realization of a solution for the screening of personalized drugs. After 24 h, spheroids were treated with different anticancer drugs; among these drugs, tamoxifen (TAM), which is the most used breast cancer drug, completely killed cells in 7 d of culture. Spheroids exhibited a drug resistance profile similar to that recognized in solid tumors. Therefore, these models are generally appropriate for solid cancer and other disease drug screening [43]. Recently, more reproducible and scalable culture platforms have been developed, such as round bottom low-attachment plate, which provide a more convenient and cheaper approach. Mukundan *et al* employed Aggrewell™400 spheroid plates to develop tumor

Table 2. Spheroids 3D *in vitro* models for breast cancer mimicry.

Fabrication	Cell density	Materials	Cells	Application	Results	References
Suspended cultures	2000 cells ml^{-1}	—	MCF7	Breast cancer drugs testing QUE and TAM killed MCF7 in 7 d	STX ↓ MCF7 growth	[43]
Suspended cultures	0.1–0.5 × 10^6 cells $well^{-1}$	Anti-adherence rinse solution	T47D	Semi-quantitative image-based tracking method with a cytometer to monitor spheroids after drugs administration	↑ area of spheroids, ↑ cell numbers per well, ↑ calcein-AM signal ↑ drug concentration, ↓ calcein-AM signal, ↓ spheroid diameter Dose-dependent ↓ spheroid area and shrinkage	[37]
Aqueous two phase	5–60 × 10^6 cells ml^{-1}	PEG-fibrinogen	MCF7 MDA-MB-231	Evaluating anticancer drugs in breast cancer spheroids	Uniformity in generation of breast cancer cells spheroids Cell viability >90% up to 14 d MCF7 formed clusters MDA-MB-231 spread and occupied the void spheres ↓ viability when MB-MDA-231 cells treated with DOX	[44]
Hanging drop	6 × 10^5 cells ml^{-1}	Agarose	MCF7 MDA-MB-231 MCF10A	Screening anticancer drugs	Drug concentration ↑, ↓ cell proliferation	[45]

(Continued.)

Table 2. (Continued.)

Liquid overlay	100 cells ul^{-1}	ACS	MDA-MB-231	Developing hydrogel system for treating breast cancer via kinetically controlled DDS	↓ volume increase in treated spheroids ↑ cell death in treated spheroids ↓ cell viability and proliferation when DOX or DOX + GEM administered	[46]
Suspended cultures	1×10^6 cells $spheroid^{-1}$	Lipid NPs for Mito delivery	MCF7	Assessment of a DDS for breast cancer therapy	Different degrees of drug penetration in the core and in the outer layers Dose-dependent response to delivered Mito	[47]
Liquid overlay	1000, 5000, 10 000 cells $spheroid^{-1}$	Agarose	MCF7 hMF hBDM	Recapitulating features of breast cancer microenvironment Platform for drug screening	MCF7 spheroids viable to 7 d ↑ cell density, necrotic core formation MCF7 + hMF + monocytes, ↑ diameter Drug efficacy ↓ in 3D models	[32]
Liquid overlay	10 000, 15 000, 30 000 cells $spheroid^{-1}$	—	MDA-MB-231 hBCAF hBM-MSC	Administration and monitoring real-time of NP for anticancer coupled with the anticancer effect of stem cells	Necrotic core for ↑ densities Co-culture ↑ cell aggregation hBCAFs secreted SDF-1α for drug resistance hBM-MSCs adhere to spheroids and invade NPs ↓ cell viability ↑ drug resistance in tri-culture	[33]
3D bioprinting	3×10^6 cells ml^{-1}	Gel and Alg (biomaterial ink)	MCF7	Quantitative drug screening method to evaluate anticancer agents effects	↑ cell viability → deposition of cells with GEL-ALG $CD44^{high}$ and $ALDH^{high}$ observed up to 9 d	[34]

(Continued.)

Table 2. (Continued.)

Fabrication	Cell density	Materials	Cells	Application	Results	References
3D bioprinting	3×10^6 cells ml^{-1}	Gel and Alg (biomaterial ink)	MCF7	Evaluating quantitatively the carcinogen-induced CSCs expression in 3D spheroids	Diameter and cell density ↑ up to 7 d ↑ CLU and NNG expression ↑ BPDE-DNA adducts	[39]
Hanging drop	625 cells ul^{-1}	—	EC hBM-MSC MCF7 MDA-MB-231	Investigating heterotypic interactions between tumor and non-cancerous cells	MDA spheroids → circular pattern up to 10 d MDA in MCF7 spheroids → ↑ cellular organization ECs formed a vasculature-like in MDA spheroids, no in MCF7 MSCs migrated in MDA-MB-231, no in MCF7 spheroids	[48]
Hanging drop	—	Agarose	hMADS MCF7 MDA-MB-231	Co-culturing breast cancer cells and adipocytes to recapitulate tumor features	↓ lipidic droplets size ↑ UCP1 in adipocytes close to tumor cells ↑ ADM receptors in hMADS ADM + UCP1 → ↑ lipolysis	[49]
3D bioprinted	50–5000 cells $spheroid^{-1}$	Hyaluronic acid (biomaterial ink)	ASC MDA-MB-231	Evaluate adipogenic behavior Investigating tumor cell-induced modulation of lipid content	ORO confirmed adipogenic differentiation after 21 d ↑ Col I, IV, VI, LAM expression and ↓ of fibronectin in differentiated constructs ↓ lipidic content of adipocytes in co-culture ↑ Col I and VI and fibronectin ↓ Col IV in co-culture	[50]

(Continued.)

Table 2. (Continued.)

Hanging drop	2×10^6 cells ml^{-1}	Agarose	MDA-MB-231	Characterizing structure and proliferation features of breast cancer spheroids Examining level of EMT Toxicity of anticancer drugs	Necrosis core up to 14 d ↑ invasion and migration in 3D spheroids E-cadherin ↓ during EMT DOX ↑ cytotoxicity	[11]
Hanging drop	75–100 cells ul^{-1}	Gel MC Type I Col (invasion assay)	4T1 67NR MDA-MB-231	Understanding how cancer clones with differential invasive skills may cooperate during invasion and metastasis	471 cells ↑ invasion in high-density COL after 2 d 67NR cells did not invade 471 able to degrade GEL layer	[51]
Suspended cultures	5×10^4 cell $spheroid^{-1}$	Matrigel	MCF10A MCF7 MCF7TR	Modeling breast cancer progression Identifying targetable alterations more like *in vivo*	Changes in chromatin due to 3D culture 3D-growth-specific looping-mediated signaling pathways in tamoxifen-resistant breast cancer cells	[3]

(Continued.)

Table 2. (Continued.)

Fabrication	Cell density	Materials	Cells	Application	Results	References
3D bioprinting	4×10^6 cells ml^{-1}	Hyaluronic acid	MCF7 Human dermal fibroblasts	Investigating the effects of the microenvironment degradation and spatial organization on breast cancer proliferation	PEG crosslinkings ↑ spatial organization Significant increase of MCF7 proliferation in well-organized structures MCF7 ↑ proliferated in presence of fibroblasts	[52]
3D bioprinting	5×10^4 cells ml^{-1}	Type I Col Thiolated hyaluronic acid	MDA-MB-231 ASC	Investigating the role of mammary adipose tissue in tumor progression	Preservation of key adipogenic markers after the bioprinting Presence of ASCs ↑ key migration parameters of MDA-MB-231	[53]

MCF7: human breast cancer cells; STX: STX64; QUE: quercetin; TAM: tamoxifen; T47D: human breast cancer cells; MDA-MB-231: human metastatic breast cancer cells; DOX: doxorubicin; MCF10A: human normal breast cells; ACS: acetyl-modified chitosan; DDS: drug delivery system; GEM: gemcitabine; NPs: nanoparticles; hMF: human mammary fibroblasts; hBDM: human blood-derived monocytes; hBCAF: human breast cancer associated fibroblasts; hBM-MSC: human derived bone-marrow mesenchymal stem cells; Gel: gelatin; Alg: alginate; EC: endothelial cells; hMADS: human mammary adipocytes; ASC: adipose stem cells; ORO: Oil Red O staining; EMT: epithelial-to-mesenchymal transition; MC: methyl cellulose; Col: collagen; 4T1, 67NR: murine breast cancer cell lines.

spheroids and investigated cell viability to monitor anticancer drugs effects in time. Results enlightened how the spheroid area is positively correlated with the number of aggregated cells and the alive signal from calcein. Moreover, by increasing drug concentrations, the alive signal decreased and so did spheroid diameters, in a dose-dependent manner [37]. Due to the urgent need to model the sustaining matrix in tumors, biomaterials have been also introduced in this approach to embed spheroids, increasing not only the model complexity, but also its reproducibility and scalability. Seeto *et al* created monodisperse microspheres composed of PEGDA covalently conjugated to a natural protein (fibrinogen) to encapsulate breast cancer cells and form spheroidal cancer microtissues. MCF7 grew in tight clusters in the microspheres, while MDA-MB-231 exhibited a more aggressive phenotype, characteristic of their metastatic nature. Moreover, the ability of these spheroids to offer a versatile platform for drug screening has been demonstrated [44]. As state-of-the-art spheroids aimed to increase the complexity and the TME mimicking, oncology research has boosted alternative routes to administer drugs or therapies. Novel chemotherapeutic drugs or agents have been researched by investigating their effects on the aggregated tumor cells in 3D spheroids. Balsa *et al* developed MCF7, MDA-MB-231, and MCF10 spheroids to screen anticancer activity and mechanisms of action of Cu(II)-acylhydrazone (CuHL) complex. This component was considered to have the potential for being a novel agent for breast cancer chemotherapy. Findings enlightened how CuHL resulted in an antiproliferative effect on both mammospheres formed with MCF7 and MDA-MB-231 cells, in a dose-dependent manner [45].

Anyway, free drugs often represent a damage for surrounding cells due to systemic toxic effects which can be induced; hence, drug delivery systems (DDSs) have been developed to bypass this drawback, by engineering carriers to drive anticancer drugs and components to specific anatomical districts. Optimization and validation of these DDSs have been performed by delivering drugs to breast cancer cells spheroids. For example, drug delivery carriers can be hydrogels, nano/micro-particles and liposomes, polymer-drug conjugates. Schneible *et al* developed a hydrogel system made of acetylated chitosan (ACS) which entrapped and then released drugs in targeted anatomical sites. Hydrogels properties can be tuned by controlling the gel fraction and crosslinking density to achieve the desired drug release kinetics, dose, and molar ratio. The *in vitro* delivery of these drugs in MDA-MB-231 spheroids demonstrated how differently the investigated anticancer drugs impacted the tumor cells: doxorubicin (DOX) significantly decreased cell viability and proliferation [46]. Similarly, Granja *et al* investigated an affordable and effective method to deliver mitoxantrone (Mito) loaded lipid nanoparticles. MCF7 spheroids were developed, and the ability of nanoparticles penetration was investigated. Fluorescent vectors showed the ability to penetrate at the outer layers of the spheroids, with some of them capable to reach the internal necrotic core; positive findings demonstrated how this DDS was able to simulate penetration ability of more effective free drugs. By considering anticancer efficacy, a dose-dependent response was observed in the treated spheroids at low concentrations; by increasing the administered dosage, Mito nanoparticles induced a higher cell death compared to free drugs at the same concentration [47].

Most of the spheroids considered in drug screening tests only comprised tumor cells, and consequently lacked mimicking cancer heterogeneity, keeping out other essential cell players of TME. Especially thanks to liquid overlay technique, co-culture of breast cancer cells and other cell lines, typically identified in pathological environment, can be performed and their relationships investigated. For example, tumor-associated macrophages and fibroblasts are frequently correlated with tumor progression and therapy resistance; for this reason, targeting these cells at the tumor site has been appointed as a promising strategy. Domingues *et al* developed multicellular spheroids by aggregating MCF7 breast cancer cells, mammary fibroblasts, and blood-derived monocytes to recapitulate features of breast TME, aiming to obtain a platform for drug screening. Triculture in these heterogeneous spheroids has been performed, forming a compact cellular structure surrounded by few cell aggregates spreading throughout the well, which corresponded to monocytes that were not able to infiltrate the multicellular spheroid. By considering the role of fibroblasts, they contributed to recruit and differentiate monocytes into macrophages, while macrophages promoted fibroblasts migration, proliferation, and trans-differentiation into myofibroblasts. The complexity of the model was shown in drug screening tests since therapeutic effects of all the tested antitumor drugs and compounds resulted in a more pronounced anticancer drugs resistance with respect to 2D cell cultures and monoculture spheroids. Diffusion distance, spatial organization, ECM production, oxygen/nutrients gradients, and cell–cell and cell-ECM interactions impacted the results of the test [32].

Alternatively, therapeutic effect of embedded stem cells (SCs) has been evaluated by Ferreira *et al*, by developing multicellular spheroids with liquid overlay technique. MDA-MB-231 metastatic breast cancer cells were co-cultured with human cancer-associated fibroblasts (CAFs). These spheroids were compact and reproducible; moreover, interactions between microtumor spheroids and nanoparticle-loaded SCs derived from bone marrow have been investigated. Findings showed how nanoparticle-loaded SCs

adhered to the external layers of the multicellular spheroids, simulating SCs affinity to the solid TME. SCs resulted able to invade the internal layers of the 3D models, even though drug resistance resulted more pronounced in multicellular 3D models than monoculture 3D spheroids [33].

3D bioprinting has been also employed to increase the degree of complexity in 3D breast cancer models, taking advantage of a supporting bioink to mimic cell-ECM interactions. Drug resistance has been investigated by Hong *et al*, who bioprinted MCF7 spheroids exploiting a printable multicomponent biomaterial formed by gelatin and alginate. These spheroids were employed to screen anticancer drugs, acting on the expression of typical drug resistance genes, as $CD44^{high}/CD24^{low}/ALDH1^{high}$, associated with breast cancer metastasis [34]. Gelatin/alginate bioinks have been further investigated more recently by Hong *et al* to generate MCF7 spheroids to quantitatively evaluate carcinogen-induced cancer SCs (CSCs) expression. CSCs are a subset of cancer cells, known as tumor-initiating cells, correlated with carcinogenesis and responsible for chemo/radiotherapy resistance. Early diagnosis of stem-like phenotypic changes associated with tumorigenesis allows more efficient cancer treatment. Breast cancer spheroids have been cultured for 7 d, increasing their diameter, area and cell density. Moreover, cells exhibited an increase of clusterin (CLU) and Nanog (NNG) expression and BPDE-DNA adducts; CLU played key role in tumor growth and metastasis, NNG represented a typical CSCs feature, while BPDE-DNA adducts meant high levels of carcinogenicity [39].

As discussed, the use of hydrogels and alternative routes for drug administration increased the complexity of spheroids and their use in oncology research. However, interactions between tumor cells and non-cancerous cells remain largely unexplored in spheroids. For this purpose, attempts to develop multicellular spheroids have been carried out. Crosstalk between non-cancerous cells (immune, fibroblasts, and mesenchymal stromal cells) has been identified as vital in driving tumor progression. Li *et al* demonstrated that the cellular composition of the model directly drove tumor biology, as CAFs and macrophages play a critical role in angiogenesis, tumor cell motility, and extravasation. They produced breast cancer spheroids by combining different cell lines: MDA-MB-231 spheroids exhibited a condensed morphology, contrarily to the more irregular shape exhibited by MCF7 mammospheres. MDA-MB-231 addition to MCF7 spheroids resulted in a better organization in the sphere architecture; moreover, endothelial cells formed a vasculature-like structure when they interacted with MDA-MB-231 metastatic tumor cells, which expressed a more aggressive phenotype, differently from less invasive MCF7, and same invasiveness behavior was observed for mesenchymal stromal cells [48].

Among non-cancerous cells, adipocytes represent a major cell population of the TME and have been recently recognized as active participants in breast cancer origin and progression. Parè *et al* co-cultured breast cancer cells with adipocytes to recapitulate TME. Co-culture demonstrated that breast cancer cells decreased the lipidic droplets size compared to adipocytic monocultures. Adipocytes in contact with mammospheres expressed uncoupling protein UCP1 and showed adrenomedullin (ADM) receptors: UCP1 expression increases lipolysis, while ADM is a multifactorial hypoxia-inducible peptide [49]. Adipocytic behavior modulated by breast cancer cells has also been investigated by Horder *et al*, who bioprinted MDA-MB-231 spheroids realized in HA on top of adipose SCs (ASCs) spheroid-laden constructs. It was demonstrated that cancer cells remained in their compartment and did not migrate into the adipose compartment; whereas Oil Red O (ORO) staining revealed a decrease in the lipidic content, associated with a cancer cell-induced reprogramming of adipocyte morphology and function. Moreover, type I and VI collagen and fibronectin accumulated in tumor models, while production of type IV collagen drastically decreased. Thus, co-culture enlightened how breast cancer cells induced characteristic alterations to adipocytes and matrix composition, demonstrating the heterotypic interaction between breast cancer cells and adipose tissue [50].

Other applications for spheroids have been intended for the investigation of the aggressive behavior of metastatic breast cancer cells, in particular the complex mechanisms of epithelial to mesenchymal transition (EMT), associated with breast cancer metastasis. During EMT, epithelial cells gradually lose cell–cell contacts, and increase their contractility, becoming motile, whereas cancer cells acquire capacity to locally degrade the matrix using invadopodia, membrane protrusions, and consequently migrate. Huang *et al* obtained MDA-MB-231 mammospheres with a compact structure up to 9 d of culture. In this model, compared to traditional 2D cultures, the level of EMT-associated proteins, like E-cadherin, resulted more significantly altered in breast cancer 3D spheroids, and aggregated breast cancer cells exhibited a higher drug resistance and higher tendence to migrate [11]. Invasivity capability was also investigated by Perrin *et al*, who developed spheroid models of breast cancer clones with different invasivity skills (4T1, 67NR) to study their invasion and metastatic behavior. The metastatic cascade is initiated when cancer cells acquire migration properties, and so they move to other anatomical districts and degrade the surrounding ECM. Both invasion and motility are commonly associated with the activation of the EMT transition, as discussed previously. Spheroids were realized by adding gelatin to cell aggregates and invasion assays were performed by embedding mammospheres in type I collagen solutions. Perrin *et al*

demonstrated that 4T1 cells proved to be more invasive when increasing the density of collagen solution, while no migration ability was observed in 67NR cells. It has been shown that metastasis ability refers primarily to the breast cancer cell lines; moreover, cells migration can be also enhanced by other cells contribute, as CAFs or CSCs. Additionally, the ECM stiffness also drives the invasion capability of breast cancer cells [51]. Li *et al* modelled breast cancer spheroids to investigate progression of MCF10, MCF7 and MDA-MB-231 cells by analyzing 3D-growth-specific looping genes. Findings showed how changes in chromatin happened due to 3D culture of breast cancer cells [3].

The research for development and application of spheroids has moved towards the aim of contemporarily increasing the complexity degree of the cell cultures and accelerating their obtainment, while maintaining a high degree of reproducibility (figure 5). At the very beginning, spheroid implementation resulted in a significant improvement in drug screening and drug resistance testing, since they ensured more accurate responses with respect to2D cell cultures, which were the main and traditional approaches used in the drugs evaluation. Recently, the urgent need to investigate the role of the surrounding matrix in tumoral niches, has progressively influenced spheroids history and evolution. Starting from more easy-to-handle processes, such as hanging drop [11, 45, 48, 49, 51] or suspended cultures [3, 37, 43, 47], the gradual introduction in oncology research of 3D bioprinting has recently triggered the involvement of this technology for the realization of spheroids [39, 52, 53]. 3D bioprinting has been implemented to answer new crucial questions related to the role of ECM on tumor progression and cancer cells organization and behavior. Borojeeni *et al* optimized the bioprinting of breast cancer models by using degradable HA hydrogels, susceptible to proteolytic degradation, crosslinked with azide modified peptides or with PEG. The influence of the biomaterial enabled the formation of spatially organized structures in presence of PEG crosslinking, which guided a greater proliferation of MCF7 breast cancer cells, especially in presence of human dermal fibroblasts [52]. The influence of the mammary adipose tissue and the crosstalk between cancer and adipose cells were investigated by Horder *et al*, by embedding MDA-MB-231 spheroids in a collagen compartment, surrounded by ASCs bioprinted in thiolated HA bioink. Interestingly, they observed how the crosstalk between MDA-MB-231 and ASCs through paracrine signals increased the migration ability of breast cancer cells to the adipose tissue compartment [53].

3D bioprinting has been implemented in spheroid realization, since it allowed the formation of cellular aggregates embedded in sustaining biomaterials, which could allow a better mimicking of the breast TME. At the same time, a higher degree of complexity could be reached by co-culturing multiple cell lines in a more standardized manner. However, the research of a more reproducible technique for spheroids has required the implementation of complex instrumentations, which definitely represents the recent drawbacks for these approaches. Additionally, 3D bioprinting has raised tremendous interest in the development of different 3D *in vitro* models, such as hydrogels, due to the tunability of their features for mimicking TME, as further discussed.

2.2. OoC models

Spheroids can be eventually placed in microfluidic chambers where culture medium exerts on spheroids shear forces and compression-induced stretches that bring spheroids closer to the *in vivo* stimuli [54]. 3D *in vitro* cell cultures, which combine different microfabrication techniques, have been developed in microfluidic 3D devices, or OoC models [55]. OoCs are microfluidic devices consisting of multi channels compatible with cell cultures which resemble physical and physiological functions of a specific organ [56]. Compared to spheroids or mammospheres, the complexity of OoCs is higher due to the coupling of approaches as soft lithography, molding, or micromachining techniques for the realization of chambers and channels [16], along with methods such as spheroids or hydrogels for the encapsulation of cells.

OoCs are produced from a complementary template (wafer) with optically clear thermoplastic materials, glass, or flexible polymers as polydimethylsiloxane (PDMS), which are casted on the template wafer and then peeled out, to monitor in real-time culture medium flow and cellular growth [56]. During the assembly of the chip, a porous membrane can be placed on the system to separate chambers and/or channels. Microchambers allow spheroids or cell-laden hydrogels to be incorporated in a confined microenvironment [9]. Microchannels, ranging around hundreds of μm [18], provide culture medium to the cells at microscale levels (figure 6), and ensure controllable mechanical stress, shear flow and concentration gradients to the cells: mechanical stimulation of cell cultures is a crucial improvement from spheroids, due to the possibility to modulate and influence cell growth in tissue development and morphogenesis.

2.2.1. Technologies for OoCs fabrication

OoCs have gained attention for breast cancer modeling due to their small size and perfused design, enabling the study of key features such as angiogenesis, intravasation, extravasation, mechanotransduction pathways, cancer cell behavior, and drug response under shear stress [9, 18]. Moreover, the use of microfluidic systems gives the opportunity to culture both single and different cell lines and to

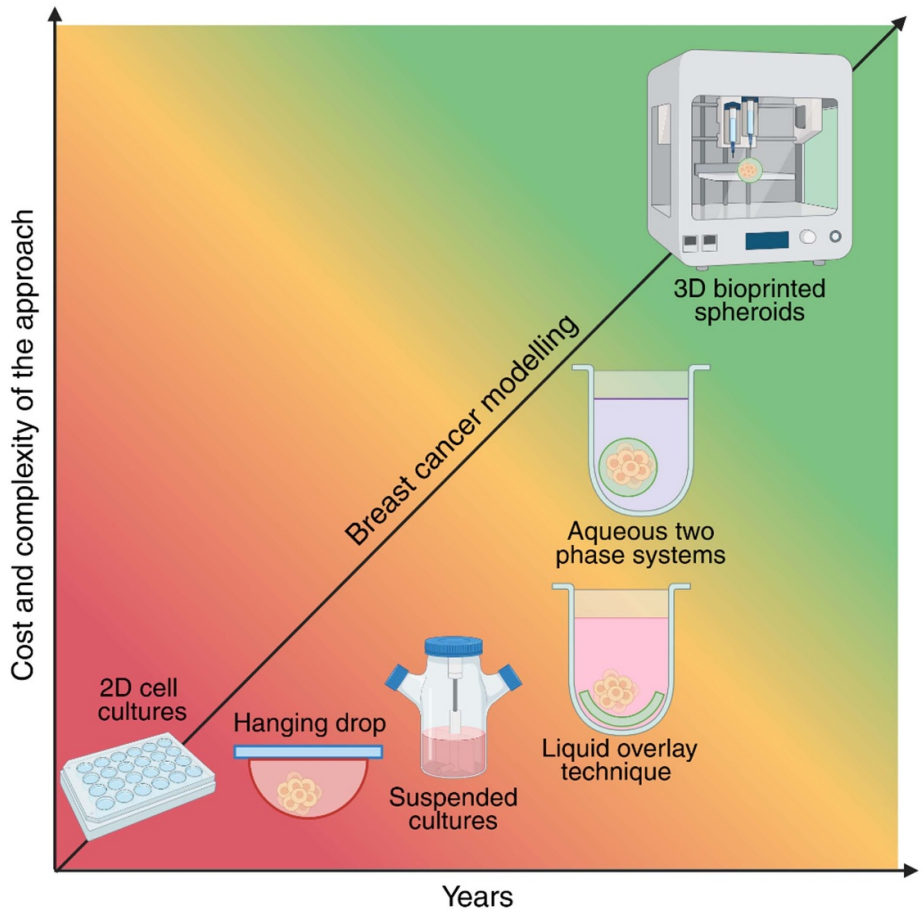

Figure 5. Evolution of spheroids for 3D breast cancer modeling. Spheroids replaced simplistic 2D cell cultures due to their better performances for drug testing. Among different methodologies, 3D bioprinted spheroids best resembled breast TME with higher degree of complexity than other approaches, but with higher costs. Created in BioRender. Unipv (2026) https://BioRender.com/ckyejap.

investigate interactions between non-malignant and cancer cells, and between tumor cells and ECM [57].

Various chip designs have been developed for OoCs [56]: single-channel chips; double-channel chips; multichannel chips. Among these configurations, double-channel chips are the most used, consisting of two separate channels connected by a porous membrane. These chips have two inlets and two outlets to control the entry and the exit of the working fluid as well as the introduction of biological materials (e.g. proteins, drugs). The porous membranes are usually made of polymeric materials, mimicking the permeability between two compartments.

Among fabrication techniques, soft lithography is applied to a wide range of materials, especially elastomers (e.g. PDMS). This method overcomes limitations of photolithography, e.g. high costs (both for the process and facilities), incompatibility with curved substrates, limited surface control, and long prototyping [56]. Briefly, a photoresist resin is patterned on a silicon wafer and exposed to ultraviolet (UV) light. PDMS, mixed with a curing agent (10:1 ratio [58],), is cast on the template and cured with a thermal cycle. The PDMS microfluidic device is hence obtained by removing it from the wafer (figure 7(A)). Alternatively, hot embossing offers an alternative for microfabrication, suitable for thermoplastic materials such as poly (methyl methacrylate) (PMMA) [56]. A template is designed and fabricated through photolithography. In the embossing machine, force and heating are consequently applied to transfer the pattern (figure 7(B)). This technique is relatively low-cost and enables high-throughput production of polymeric microstructures, though precise temperature control is required. Injection molding technique is an alternative approach to microfabricate OoCs (figure 7(C)). Advantages in using injection molding are related to the low costs, which are restricted to the fabrication of the template. Many micro-devices can be produced with this method (e.g. sampling cells, micro-heat exchangers, lab-on-chip packages) [56]. However, the fabrication process is very complex and laborious, whereas temperature, pressure and injection rate must be finely controlled to ensure production quality. Finally, 3D printing is an emerging method to obtain low-cost and efficient templates, components, and devices at the microscale [56] (figure 7(D)). Advantages are linked to its rapid prototyping, precise control, and application of the desired cell arrangement. However, 3D printing can

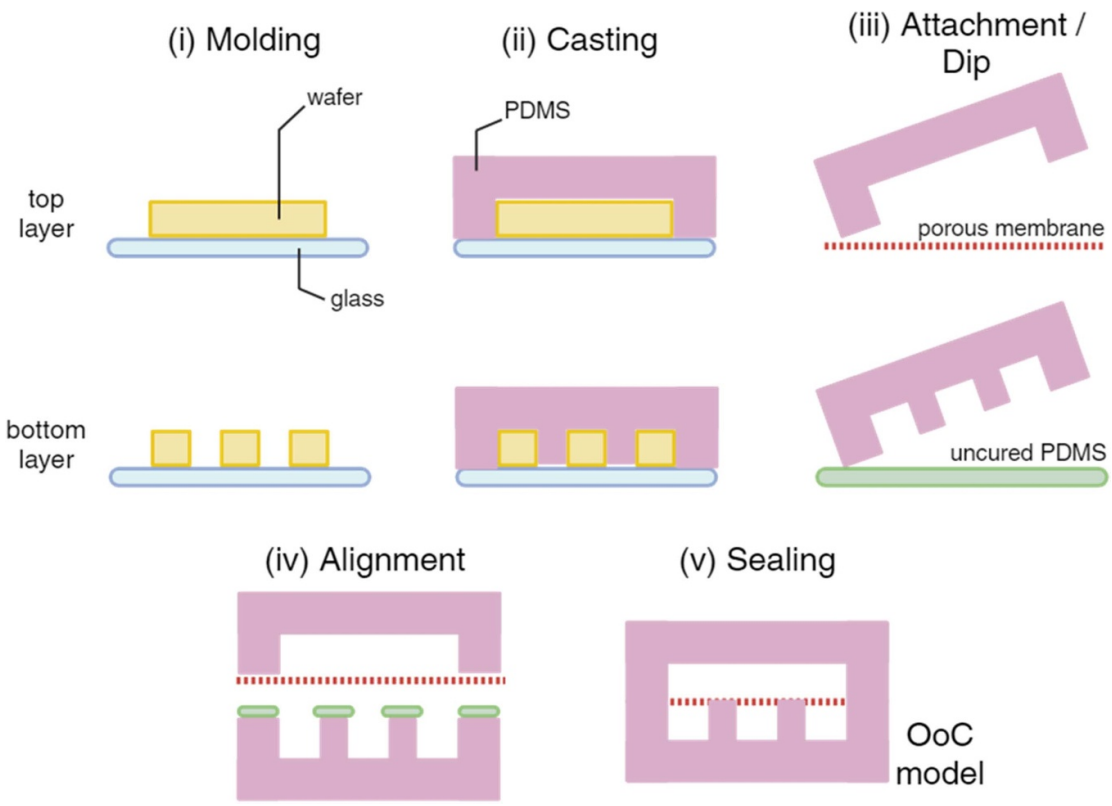

Figure 6. General process for OoCs fabrication. The technique for obtaining the final microchip depends on the material: casting phase and subsequent removing refer to PDMS OoC models. Created in BioRender. Pitton (2026) https://BioRender.com/1kl7i25.

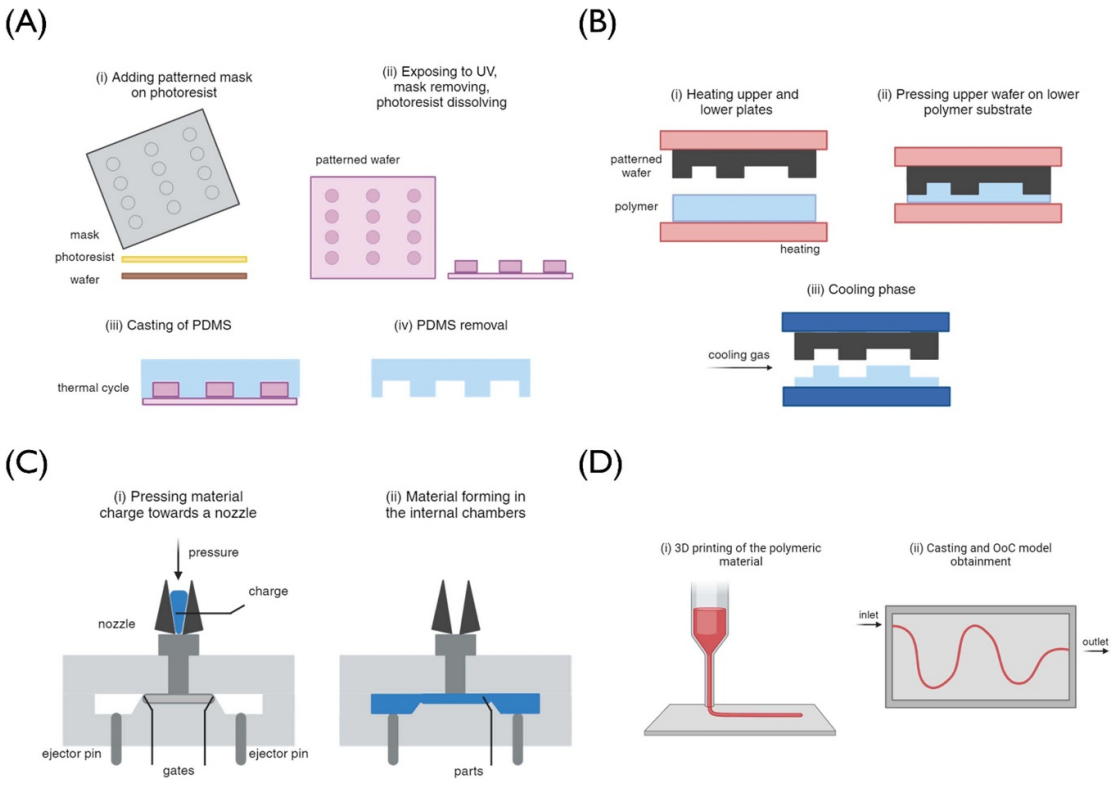

Figure 7. Technologies for OoCs formation by casting/pressing/printing materials on a template wafer. (A) Soft lithography. (B) Hot embossing. (C) Injection molding. (D) 3D printing. Created in BioRender. Pitton (2026) https:// BioRender.com/0h96w91. Created in BioRender. Pitton (2026) https://BioRender.com/3gv61k2. Created in BioRender. Pitton (2026) https://BioRender.com/lbjuvqk. Created in BioRender. Pitton (2026) https://BioRender.com/awic83t.

be limited due to its low resolution (about 350 μm) and its compatibility only with certain materials.

Main features and advantages/disadvantages of OoCs fabrication technologies (figure 7) are summarized in table 3. Generally, advantages in the use of OoC microfluidic devices for breast cancer 3D models include [15, 18, 58, 59]: possibility to manipulate microfluidic amounts of fluids via microchannels; possibility to culture cells in microchambers; precise control on ECM, as mechanical/chemical factors, cell composition, and medium flow; great reproducibility, sensitivity and accuracy; capacity for large-scale production; rapid experimental outcomes; low costs.

2.2.2. State-of-the-art OoCs and their evolution

OoCs applications in breast cancer modeling (table 4) have enabled the investigation of tumor cell behavior across different stages of disease progression. It is well-known that breast cancer cell lines show different behaviors and aggressive tendencies depending on their nature. Jouybar *et al* demonstrated that human breast cancer cell line MCF7 exhibits less aggressive behavior compared to the metastatic MDA-MB-231 line. Breast cancer spheroids were realized by encapsulating tumor cells in Matrigel droplets at the cold inlet of the microfluidic device (3 °C–4 °C); subsequently, cells were transported in the warm portion of the chip (37 °C), where Matrigel gelled and formed cell-laden microbeads with fluorinated oil.

These microbeads were sandwiched between two collagen layers, creating a heterogeneous collagenous ECM. MCF7 cells remained poorly aggressive and low-invasive, and remained in their initial conformation, arresting their proliferation in a microtumor, whereas MDA-MB-231, recognized as highly metastatic, gradually invaded the surrounding matrix, exhibiting single cell invasion, without a fully directional motion. These findings evidenced how the former could resemble early stage of breast cancer, known as ductal *in situ* carcinoma, since the cancer mass remains stable in a confined microenvironment, without invasion; contrarily, the latter represented a faithful model of more aggressive pathology, as invasive ductal carcinoma [60] (figure 8(A)).

Invasiveness of breast cancer cells is strongly influenced by the features of the matrix. Lam *et al* investigated the administration of nanoCaCO$_3$ particles on the dynamic kinetic of metastatic MDA-MB-231 cells. The OoC was realized by separating two upper and two lower tissue chambers, representing treatment and control condition, respectively; adjacent chambers were fabricated with fibrin, to simulate the ECM, while an internal channel worked to provide and collect culture medium. The treatment consisted in administering acid-neutralizing nanoCaCO$_3$ particles to breast cancer cells at different concentrations, characterized by high payload and buffering capacity; concentrations higher than 0.2 mg ml^{-1} resulted enough to inhibit tumor growth after 5 d of cell culture. Contrarily, nanoCaCO$_3$ particles were demonstrated not to affect the growth ratio of fibroblasts, co-cultured with cancer cells, enlightening how nanoparticles selectively inhibit tumor growth [61] (figure 8(B)). Lugo-Cintròn *et al* investigated the effect of the density of a collagenous ECM on the functionality of metastatic MDA-MB-231 cells; ECM density represents another key feature in cell growth and invasion ability. Additionally, cancer cells can interact with other components of the TME, such as blood or lymphatic vessels, which provide a route for cancer cells metastasis and intravasation, causing matrix remodeling. For this purpose, a metastasis-on-chip (MoC) was realized using a microfluidic device which incorporated a central lymphatic vessel cultured in the collagenous ECM. The density of the matrix varied using low-density collagen (i.e. 3 mg ml^{-1}, normal breast tissue) and high-density collagen (i.e. 6 mg ml^{-1}, cancerous breast tissue). Human lymphatic endothelial cells (HLECs) were seeded in the lumen of the central vessel; no morphological changes were noticed in the two differently concentrated ECM. Contrarily, specific inflammatory cytokines, secreted from endothelial cells, increased in high density matrix: cytokine IL-6 is a key player of cell dysfunction and tumor progression, and was the most strongly upregulated one (i.e. 3-fold increase in high density matrix). Interestingly, the disruptive effect of cytokine IL-6 increased in co-culture of HLECs and MDA-MB-231, both in denser and weaker ECM [62] (figure 8(C)).

MoCs represent powerful systems to evaluate the behavior of metastatic cancer cell lines during migration and invasion to other anatomical districts. Breast cancer cells mostly metastasize in lungs, liver, bone, brain, and lymph nodes (Banerjee and Devi Rajeswari, 2023). Interactions between breast cancer cell lines (MDA-MB-231 spheroids, and spheroids of MDA-1833 bone tropic breast cancer cells), neurons (SH-SY5Y) and bone cells (PBMCs) have been investigated by Conçeicao *et al*, who developed a MoC composed of a top slab, with three patterned cell compartments and channels, a bottom slab with valve structures and a membrane in between. Breast cancer cells expressed a plethora of pro-inflammatory factors, as IL-11 secretion increased in MDA-1833 compartment, suggesting that culturing cells in MoC enhanced the aggressive phenotype of breast cancer cells. By culturing all three cell lines together, a pro-inflammatory phenotype was observed in the breast cancer compartment, where the level of IL-6 and MIP-1α augmented. Sympathetic stimulus thus enhanced these cytokine levels, both in MDA-MB-231 and MD-1833 cells [63] (figure 8(D)).

Dynamic co-culture systems in OoCs provide a platform to assess tumor–stromal interactions and evaluate anticancer therapies. Ozer *et al* Used the OrganoPlate® platform to develop a OoC which mimicked cancer metastasis and performed a drug

Table 3. Resolution, time scale, costs, advantages and disadvantages of the fabrication technologies for OoCs.

Method	Resolution (μm)	Time scale	Costs	Advantages	Disadvantages
Soft lithography	3–250	Fast	Relatively low	Improvements of photo-lithography limitations	Absorption of hydrophobic molecules due to PDMS
Hot embossing	40–100	Slow	Relatively low	Resistance to pressure and to temperature fluctuations	Precise control of temperature Need of master mold fabrication
Injection molding	100–400	Complex and laborious	Low	High precision fabrication (*limited to the master*)	Process parameters must be optimized Need of master mold fabrication
3D printing	>350	Fast	Relatively low	Precise control and desired cell arrangement	Inadequate optical transparency No compatibility with all the materials

profile screening of anticancer drugs for pre-clinical drug testing and screening. This microfluidic device showed a 3-lane design, with a cancer channel (MDA-MB-231, MCF7), a micro-vessel perfusion channel (with human umbilical vein endothelial cells, HUVECs) and a surrounding gel of type I collagen and fibronectin. Cancer compartment simulated the pathological ECM, and breast cancer cells were co-cultured with stromal fibroblasts. MDA-MB-231 cells invaded the ECM gel towards micro-vessels, with a higher degree of motion when co-cultured with fibroblasts; contrarily, MCF7 remained incapable of invading ECM gel. By optimizing cell lines population, the OoC has been implemented as a platform for drug screening, by monitoring cell proliferation, migration, invasion, tumor cells number, intravasation and endothelial cells number. Several anticancer drugs were investigated [64] (figure 8(E)). The non-cancerous microenvironment is thus responsible for forming ECM with a key role in carcinogenesis, and relationships between tumor cells and stromal cells remain unrevealed in anticancer therapies. It is well known that the presence of different cell populations allows to simulate the interaction of breast cancer cells with other typical stromal cells, as fibroblasts, vascular networks, endothelial and epithelial cells, aiming to resemble TME and evaluate tumor behavior and screen anticancer drugs. Flont *et al* developed an OoC with two PDMS layers and a porous PET membrane to co-culture in two distinct layers breast cancer cells (MCF7) and fibroblasts (HMFs). The cytotoxicity of DOX was examined. Viability of fibroblasts and breast cancer cells decreased by enhancing the concentration of DOX [70] (figure 8(F)). Moreover, the advantages in the use of microfluidic devices to culture breast cancer cells were exploited for the possibility of developing a patient personalized anticancer therapy. Prince *et al* realized a platform for culturing breast cancer cells spheroids which can serve as an *in vitro* preclinical model for effective screening of new anticancer drugs. Cancer spheroids (MCF7) were realized in a gelatin and cellulose hydrogel and seeded as gelling droplets in multiple parallel rows of the microfluidic array, replicating the dense fibrotic nature of breast TME. Two anticancer drugs, DOX and 4-hydroxytamoxifen, were evaluated, reducing spheroid viability by 34% and 23%, respectively [65] (figure 8(G)).

Integration of microvasculature within OoCs enhances physiological relevance by reproducing the abnormal vascular networks characteristic of tumors. Chi *et al* employed L-TumorChip, a microfluidic device which emulates tumor–stroma complexities and tumor-endothelium interactions, particularly breast cancer cells invasion. The OoC was composed of a top channel seeded with human microvascular endothelial cells (HMVECs) and a lower compartment, realized with MDA-MB-231 breast cancer cells and CAFs in Matrigel; the two portions were divided by a porous membrane. The relationship between stromal cells and cancer cells growth was investigated, as well as the stromal effect on drug responses. In particular, the endothelial monolayer showed a higher permeability than normal vasculature after 2 d of culture; this finding can be attributed to the cancer cells behavior, which altered permeability with the secretion of growth factors (VEGFs), cytokines, and chemokines The endothelial layer exhibited increased permeability after two days, attributed to cancer cell–derived VEGFs, cytokines, and chemokines [10] (figure 8(H)). Similarly, Nashimoto *et al* incorporated an engineered vascular network (HUVECs) within

Table 4. OoC 3D *in vitro* models for breast cancer mimicry.

Fabrication	OoC dimensions	Materials	Cells	Application	Results	References
OoC devices for culturing cell-laden Matrigel droplets embedded in collagen	$D = 16, 50, 67$ μm (microbeads) $D = 500$ μm (channels)	SU-8 (wafer) PDMS (chip) Matrigel (hydrogel beads) Col (ECM)	MCF7 MDA-MB-231 MCF-10A	Investigation of a pre-invasive breast cancer model in a heterogeneous ECM	Cell-laden beads enveloped in collagen for invasion assay MCF7 remained in the initial state (DCIS state), MDA-MB-231 invaded matrix (IDC state)	[60]
OoC with 2 upper and lower chambers, with adjacent chambers to measure cell migration	$V = 0.61$ mm^3 (tissue chambers) $V = 0.015$ mm^3 (chambers)	SU-8 (wafer) PDMS (chip)	MDA-MB-231 Fibroblasts	Monitoring tumor growth by treating cells with or without nanoCaCO$_3$ (<120 nm) particles	nanoCaCO$_3$ ↑ extracellular pH to 7.4, inhibit tumor growth and migration	[61]
OoC microfluidic model consisting of two PDMS layers, as microchambers	—	SU-8 (wafer) PDMS (chamber) Col (ECM)	HLEC MDA-MB-231	Recreating luminal geometry to investigate effects of ECM density and lymphatic metastasis	↑ proliferative phenotype and pro-inflammatory secretion profile in high density matrix	[62]
OoC with a top slab for cell compartments and diffusion channels, a bottom slab with valve structures + membrane	$D = 6$ mm (cell compartments) $L = 4.5$ mm, $D = 300$ μm, $h = 150$ μm (channels)	Gray V4 resin (wafer) PDMS Matrigel (spheroids)	CD14$^+$ PBMC MDA-MB-231 MDA-1833 SH-SY5Y	Reproducing the dynamic crosstalk between breast cells and bone cells	Model of breast cancer in a bone metastatic context Platform for drug screening Incorporation of patient derived cells	[63]
OoC (OrganoPlate) platform 3-lane design to optimize a MoC, with ECM and vessels compartments	—	OrganoPlate chip Col, FN (ECM)	HUVEC Fibroblasts MCF7 MDA-MB-231	Mimicking the early stages of cancer metastasis Drug profiling screen of anticancer drug	Co-culture produced invasive response of MDA-MB-231 Anticancer drugs inhibited cells invasion and intravasation	[64]
OoC with 6 PET porous membranes between co-cultures of non-malignant and cancer cells	$D = 50$ μm (microchannels) $D = 1$ cm (PET membrane) $V = 15\,000$ mm^3 (PDMS)	PET (membrane) PDMS (chip)	HMF MCF7	Co-culturing non-malignant and cancer cells Integration of a porous PET membrane for drug testing	Regular and reproducible cell culture Studying drug screening and diffusion Test membrane penetration	[57]

(Continued.)

Table 4. (Continued.)

Fabrication	OoC dimensions	Materials	Cells	Application	Results	References
OoC for studies the response of tumor spheroids to different anticancer drugs	$A = 1.2 \times 3$ cm (microfluidic device)	SU-8 (wafer) PDMS (chip) Gel, CNC (hydrogels)	MCF7	*In vitro* model for personalized cancer therapy and screening of anticancer drugs	Uniform distribution of drugs Oxygen and nutrient gradients mimicking the *in vivo* tumor ↑ flow rates, ↑ drug assumption	[65]
OoC (L-TumorChip) with 3-layered PDMS array, composed of tumor compartments and endothelial layer	$h = 150$ μm (channel) $R = 490$ μm, $h = 200$ μm (chamber)	PDMS (chip, membrane) Matrigel (cell culture)	HMVEC CAF MDA-MB-231	Emulating heterogeneity Mimicking cancer invasion and angiogenesis Real-time drug response	The OoC mimicked endothelium barrier and the tumor heterogeneity Monitoring the dynamic drug response in real time	[10]
OoC with 3 layers, a top layer with microfluidic channels, a bottom membrane, and a glass slide	$D = 2$ (microchannels) $D = 1$ mm (microchambers)	SU-8 (wafer) PDMS (microchannels, membrane)	HUVEC hLF MCF7 SW60 HepG2	Developing a tumor spheroid integrating vascular network	↑ proliferation of MCF7 No dose-dependent decreases in tumor cells from anticancer drugs	[66]
OoC for spheroid-in-gel culture, to pattern lanes of hydrogel	$h = 30$ μm (lines)	PDMS Col (spheroids)	HUVEC hLF MCF7	Obtaining cancer spheroids in an endothelial cells-laden hydrogel to test anticancer drugs	Integrating on-chip spheroid formation and in-place gel encapsulation	[67]
OoC to grow tumor spheroids and bioengineered vessels		PDMS (chip) Matrigel and type I Col (ECM)	HUVEC MDA-MB-231 HLF, MSC	Vascularization of solid tumor *in vitro*	Col presence in ECM allowed HUVECs to not collapse Matrigel ↑ invasiveness	[68]

(Continued.)

Table 4. (Continued.)

OoC with 6 pillars microstructures for bioprinting a 4 × 10 array of cell-laden hydrogels	$h = 200\ \mu$m (microchannels)	SU-8 (wafer) PDMS (chip) Alginate/fibrin (bioink)	HUVEC BT474	Creating multiple TME models Self-organizing a vascular barrier surrounding each spheroid	Self-organized TME High viability of cells up to 7 d of culture	[58]
OoC with bilayer hydrogel incorporated in a microfluidic device	$D = 1$ mm (hydrogel)	NR9 (wafer) PDMS (chip) GelMA (hydrogel layers)	MCF7 MDA-MB-231 HUVEC THP-1	Investigating T-cells extravasation Evaluating the effects of hypoxia condition	T-cells extravasated in breast cancer spheroids Cancer spheroids ↑ hypoxia than dispersed cells	[69]

D: diameter; PDMS: polydimethylsiloxane; Col: collagen; ECM: extracellular matrix; MCF7: human breast cancer cells; MDA-MB-231: human metastatic breast cancer cells; MCF10A: human normal breast cells; DCIS: ductal *in situ* carcinoma; IDC: invasive ductal carcinoma; V: volume; HLEC: human lymphatic endothelial cells; L: length; h: height; $CD14^{+}$: human monocytes; PBMC: peripheral blood mononuclear cells; MDA-1833: tropic breast cancer cells; SH-SY5Y: neural cells; FN: fibronectin; HUVEC: human umbilical vein endothelial cells; PET: polyethylene terephthalate; hMF: human mammary fibroblasts; A: area; Gel: gelatin; CNC: cellulose nanocrystals; R: radius; HMVEC: human microvascular endothelial cells; CAF: cancer associated fibroblasts; hLF: human lung fibroblasts; SW60: human colon cancer line; HepG2: hepatocellular carcinoma cells; MSC: human mesenchymal stem cells; BT474: breast cancer cells; THP-1: immune cells; GelMA: methacrylate gelatin.

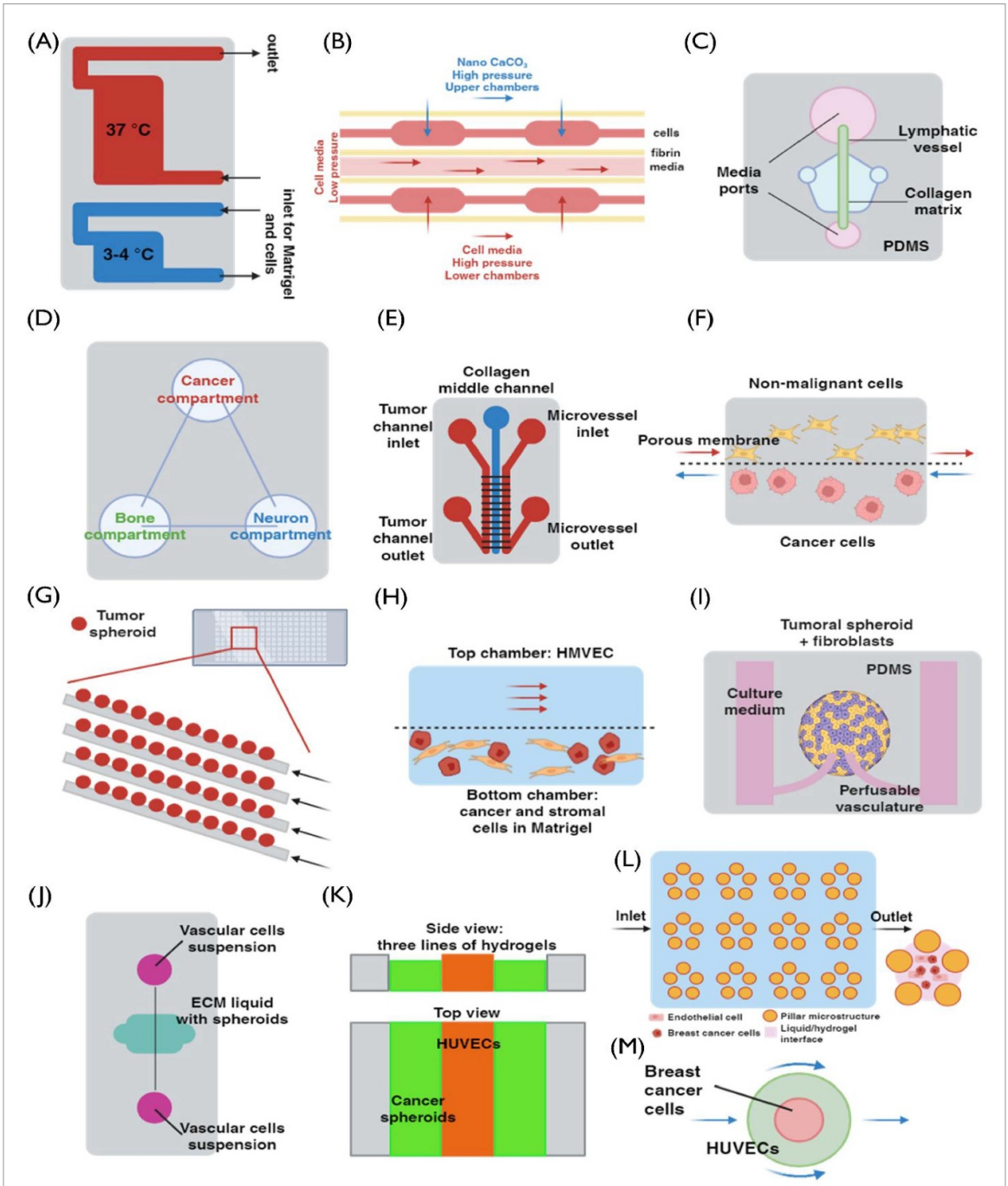

Figure 8. Schematic illustration of mentioned OoCs models. (A) OoC for studying breast cancer cells behavior at different stages of the pathology. (B)–(C)–(D) OoCs for the evaluation of the breast cancer cells invasiveness. (E)–(F)–(G) OoCs for the screening of anticancer drugs. (H)–(I)–(J)–(K)–(L) OoCs with integrated internal microvasculature for drug screening and cell–cell interactions. (M) OoC for investigation of trivial conditions of breast cancer tumorigenesis. (A)–(F) Created in BioRender. Pitton (2026)https://BioRender.com/2ly8c14. (G)–(M) Created in BioRender. Pitton (2026)https://BioRender.com/zj9maqa.

breast cancer spheroids (MCF7), suspended in fibrin/collagen gel with lung fibroblasts (hLFs), developing an OoC which can maintain perfusion for over 24 h. It was demonstrated that monoculture did not induce any sprouts in the microfluidic device, while co-culture (hLFs and MCF7) evidenced a growth of fibroblasts in the core surrounded by cancer cells; in tri-culture, MCF7 spheroids increased in diameter and formed large hollow structures, as vasculature-like structures. The effects of PAC, an anticancer drug, were investigated; it was observed that volume of spheroids decreased in a dose-dependent manner [66] (figure 8(I)).

The incorporation of a vascular network and blood flow can closely resemble the process of tumorigenesis. Kwak *et al* fabricated an OoC to investigate interactions between tumor spheroids and perfused blood vessels, observing the integrity of HUVECs vascular lumen, the sprouting behavior of tumor MDA-MB-231 spheroids, angiogenesis, and vascular invasion. MDA-MB-231 spheroids were prepared and inserted in the chip chambers with ECM-like

materials, such as type I collagen, Matrigel, or fibrinogen; then, HUVECs were seeded in the internal channels. HUVECs vasculature did not collapse in collagen matrix, but collagen-rich ECM did not promote any sprouts from tumor spheroids, that did not ensure proper stability of the vasculature. Moreover, fibroblasts were co-cultured with ECs and breast cancer cells in fibrinogen matrix, and active sprouting of MDA-MB-231 was observed during 6 d of cell culture [68] (figure 8(J)).

Su *et al* performed a cancer spheroid culture in a microarray chip by using hanging drop method for the embedding of spheroids in hydrogels and confinement in the OoC. Each spheroid was encapsulated on-chip in type I collagen hydrogels; subsequently, spheroids were co-cultured with HUVECs in fibronectin to form a vascular network surrounding the tumor cell culture. Administration of paclitaxel demonstrated that the higher the concentration of drug, the higher the death rate for cultured cancer cells Su *et al* employed a microarray chip based on the hanging-drop method to culture tumor spheroids encapsulated in type I collagen hydrogels. Co-culture with HUVECs within fibronectin promoted vascular network formation around the tumor spheroids. Treatment with paclitaxel induced a dose-dependent increase in cancer cell death, demonstrating the model's utility for drug evaluation [67] (figure 8(K)). A self-organizing vascular endothelial barrier surrounding tumor spheroids was developed by Lee *et al*, who coupled bioprinting techniques to produce spheroids and the incorporation of a microfluidic device. A bioink composed of RGD–alginate and fibrin, loaded with BT474 breast cancer cells and HUVECs, was bioprinted into microfluidic chambers with precise spatial control. It has been observed that HUVECs formed a vascular barrier at the liquid-ECM interface by migrating towards the gel, while BT474 formed spheroids with a gradual aggregation up to 7 d of culture [58] (figure 8(L)).

OoCs have been also developed to investigate trivial conditions of breast cancer tumorigenesis, such as immune cells (T-cells) infiltration and hypoxia conditions. Aung *et al* fabricated an OoC composed of a bilayer gelatin methacrylate (GelMA) hydrogel to separately co-culture breast cancer (MCF7, MDA-MB.231) and immune cells (THP-1), encapsulated in the inner layer, and HUVECs, in the outer layer, in a microfluidic device. 3D micropatterning techniques have been used to separate the different cell types within the hydrogel. Hypoxia was simulated by culturing cancer spheroids or dispersed cancer cells. It was observed that T-cells perfused in the chip were preferentially recruited from breast cancer spheroids with higher hypoxic conditions compared to dispersed cultured breast cancer cells. Moreover, the presence of monocytes in the inner layer enhanced T-cells extravasation into the core of the cell culture [69] (figure 8(M)).

Over the years, OoC design has evolved in response to the growing needs of oncology research. Initially, microfluidic systems were introduced in 3D models to reproduce different human tissue compartments interconnected by microchannels. This compartmentalization represented a key advantage of OoCs, enabling simulation of organ-level communication and microcirculation (figure 9). Beyond modeling static spheroids for drug screening, the integration of internal microvasculature became essential to mimic the physiological breast TME, where vascularization drives cancer cell migration and metastasis. Early OoC models were relatively simple [62, 65], more sophisticated models were recently fabricated with scalable structures [58] or with embedded biomaterials, since OoCs lacked the presence of a sustaining TME but recent systems incorporate scalable architectures [58] and biofunctional materials that better replicate the supportive TME [60, 64, 71]. From single OoCs, new technologies implemented double or multichannel OoCs, which guaranteed a higher degree of complexity with respect to primitive OoCs (and spheroids as well), and more complex approaches were exploited for a more scalable fabrication (e.g. 3D printing). Coupling spheroids and OoCs could eventually address unsolved issues, due to the tumor-like conformation of cell aggregates in spheroids and micro-circulation in OoCs [66, 67]. Moreover, OoCs tried to satisfy all those objectives which remained limited in spheroids due to their drawbacks, e.g. the study of invasiveness and migration of the breast cancer cells and the evaluation of the eventual crosstalk between breast cancer cells and stromal cells in an engineered TME. This final aim agrees with the major clinical need we are stressing in this review, since the importance of the role covered by TME in cancer progression is nowadays clear and has dramatically guided the oncology research. In OoCs, it is evident how complex microfluidic systems with ECM-like microchambers have been more recently designed and developed for assessing the role of TME on cell behavior, as previously discussed. Although higher complexity degrees could be achieved by implementing novel technologies for OoCs, high costs and low-handling ability in sustaining recent instrumentations could severely decrease the interest of oncology research in OoCs.

2.3. Engineered 3D constructs

The choice of the proper supporting biomaterial is crucial in Tissue Engineering approaches, as the biomaterial provides cells with an adequate engineered matrix which resembles the native ECM. Biomaterials involved in the development of engineered 3D constructs can be natural-derived polymers, including collagen, gelatin, HA, alginate, silk fibroin, chitosan, and decellularized ECM (dECM), or synthetic polymers, including PEG, polylactic acid, polycaprolactone (PCL), polyurethane, and Pluronic F127.

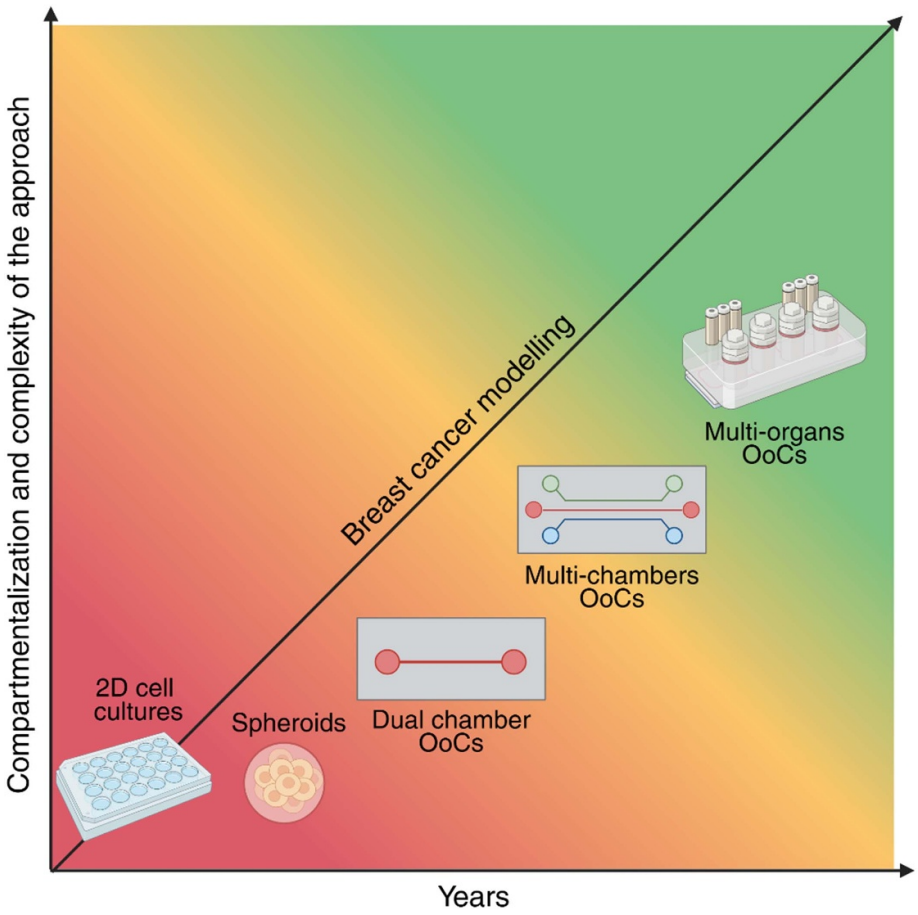

Figure 9. Evolution of OoCs for 3D breast cancer modeling. OoCs were introduced to implement compartmentalization and respond to the necessity to investigate features of breast cancer, e.g. EMT, metastasis. OoCs were progressively augmented in terms of complexity, despite increasing costs and time of realization. Created in BioRender. Unipv (2026) https://BioRender.com/jhg6q6p.

Each class presents distinct advantages and limitations. Natural-derived polymers, being structurally and chemically similar to native ECM components, exhibit excellent biocompatibility and biodegradability, supporting cell adhesion, proliferation, and differentiation. However, they often suffer from batch-to-batch variability, poor mechanical strength, and rapid degradation in physiological environments, which can compromise reproducibility and influence cell behavior [72]. Contrarily, synthetic polymers can be synthesized in a controlled and well-organized manner, and physical and mechanical features, such as stiffness, degradation kinetic, hydrophobicity, morphology, and porosity are achieved with elevated reproducibility and low variability. Still, synthetic biomaterials lack bioactive groups [73], which characterize healthy or pathological ECM, and require surface chemical modification.

2.3.1. Technologies for engineered 3D constructs fabrication

Recently, engineered 3D constructs have gained attention to resemble *in vitro* breast TME: scaffold-based, hydrogel-based and bioprinted models have thus been developed with modern approaches of AM, aiming to generate versatile 3D platforms to resemble tumor heterogeneity and to test novel anticancer therapies.

Scaffold-based models provide a solid and stable 3D structure as a substrate for culturing breast cancer cells, which are seeded onto the external surface of the scaffold through pipetting or dynamic culture systems [9]. The porosity and interconnectivity of the scaffold are critical, as cells must infiltrate and colonize the internal structure to reach the core. Hydrogel-based models allow cell encapsulation directly into their polymeric network, prior to the process of crosslinking, necessary for structure stabilization. The possibility to directly embed cells into hydrogels represents the main difference and the crucial advantage of these models with respect to scaffolds [72]. Bioprinted models are obtained by 3D bioprinting of cell-laden hydrogels (*bioinks*) and have recently gained tremendous attention for reproducing breast cancer TME due to the possibility to finely control the arrangement of the deposited material [74]. Bioinks must be optimized in terms of viscosity to ensure proper printability during the printing process and then crosslinked to guarantee physical integrity and mechanical stability for long-term cell cultures. The

denomination *bio*ink derives from the fact that the cells are directly embedded in the material prior to the printing, allowing to deposit them homogeneously throughout the whole structure and to halve the time of realization by joining the realization of the structure and the inclusion of cells in a single procedure. By taking advantage of this feature typical of hydrogel-based models, it is possible to scale up to a large and consistent production of 3D bioprinted models.

The design and development of engineered 3D models must respect some defined criteria regarding [75] scaffold architecture; mechanical features; degradation kinetic; biological properties. A promising engineered 3D structure must exploit these features to ensure cells *feel* a sustaining matrix which resembles as better as possible the characteristics of the *in vivo* tissue.

Scaffold architecture must comprise high porosity and interconnected pores. The size of the pores must be suitable for nutrients/oxygen/waste products exchanges and cell infiltration (scaffold-based) or cell movements and adaptation (hydrogel-based, bioinks) [75]. As such, too small pores impact cell migration, while too large pores reduce cell adhesion due to low available scaffold surface. Moreover, the choice of the breast cancer cell line is also crucial due to the fact that cell growth can be affected by the pore dimensions. As reported in literature, MCF7 breast cancer cells exhibit an average diameter equal to 16–25 μm, while MDA-MB-231 metastatic breast cancer cells show a mean dimension of 15.81 μm [75]. The ideal porosity of engineered 3D models must range from 50 to 300 μm, to initially promote cell attachment and consequently tissue maturation [76].

Mechanical properties are equally critical, as matrix stiffness influences cell behavior and tumor progression. Engineered 3D models should mimic the mechanical characteristics of breast tissues at various pathological stages. However, no standardized stiffness range has been established, due to patient variability (age, anatomy, tumor stage) and methodological differences in tissue testing (e.g. magnetic resonance elastography, dynamic compression, nanoindentation). Reported data indicate that breast tumor cores typically exhibit stiffness values below 1 kPa, whereas surrounding matrices exceed 1 kPa [75]. Increased stiffness has been measured in aggressive HER2+ and TNBC (triple negative) breast tumors, whereas decreased stiffness in luminal tumors. During the pathology progression, ECM remodeling plays a pivotal role in altering the features of the TME; in a diseased woman, invasive ductal carcinoma leads to a 3-fold increase in tissues stiffness with respect to healthy adipose tissue, and to 1.5 times increase if compared to healthy glandular tissue. In conclusion, even though mechanical properties of breast cancer have not been defined yet, it seems clear that pathological tissues result in higher values of stiffness which are conferred by the cancer-derived mutations induced by breast cancer cells to non-cancerous cells and to the surrounding matrix components, such as elastin, collagen, and proteoglycans. Mechanical properties of pathological tissue hence result higher than in healthy tissues: fibroadenomas are 2 times stiffer than normal breast tissues, fibrocystic diseases and malignant tumors are 6 and 3–6 times stiffer, respectively; invasive carcinoma results the stiffest tissue, with an increase in elasticity 13 times than the normal tissues (table 5), specifying the techniques used for the analysis.

Regarding kinetic degradation, 3D constructs must guarantee long-term stability during cell culture (i.e. a minimum of 2 weeks [75]). The stability of the developed constructs is directly associated with the degree of crosslinking of the material, which ensures a proper water uptake which regulates the exchanges of culture medium between cells and matrix. Large polymeric networks allow a huge flux of nutrients/oxygen/waste products on one side but consequently generate a more pronounced swelling ability which might promote their biodegradation.

All physical and mechanical features are combined to promote cells behavior onto or into the 3D model. The selected biomaterials, or multicomponent biomaterials, must offer a bioactive platform to promote cell adhesion, growth, and proliferation. Moreover, cells must exhibit the peculiar characteristics of their natural line, like differentiation and metastasis/invasion. As already described, natural biomaterials can present in their polymeric structure the typical binding motifs (RGD motifs), to enhance cells adhesion; contrarily, non-adhesive natural and synthetic polymers can be finely functionalized by decorating their structures with adhesive moieties or by incorporating an adhesive biomaterial. However, the criteria of biocompatibility must be strictly respected by engineered 3D constructs.

2.3.2. Scaffold-based models or bulk scaffolds

Scaffold-based models or bulk scaffolds are usually investigated to reproduce migration, invasion, and metastasis of breast cancer cells [9]. Cells are directly seeded *onto* the surface of the fabricated model and gradually proliferate in the internal cavities of the structure by taking advantage of its porosity. Adhesion can be favored by adhesion motifs possessed by the biomaterial, which can also change cellular gene expression and signal transmission [82]. The main advantage of scaffold-based models is associated with their macro-porosities, characterized by a high interconnectivity to best mimic breast cancer invasion and metastasis (table 6) [83]. Scaffold-based models can be obtained with approaches such as freeze-drying, particulate leaching, and cryo-polymerization. Alternatively, modern approaches of AM can be employed, mainly using 3D printing.

Advantages of freeze-drying or lyophilization (figure 10(A)) can be associated with the easy process

Table 5. Results of the calculated stiffness (in terms of elastic modulus) of breast tissues, by using different techniques, reported in literature.

Technique	Portion of tissues	Elastic modulus (kPa)	References
Magnetic resonance	Adipose tissue	0.43 ± 0.07	[77]
	Glandular tissue	2.45 ± 0.20	
	Adipose tissue	4–16	[78]
	Breast cancer	18–94	
Tomographic elastography	Adipose tissue	4.17 ± 0.07	[79]
	Benign breast cancer	9.03 ± 0.22	
	Malignant breast cancer	16.45 ± 1.10	
Nanoindentation tests	Adipose tissue	3.25 ± 0.91	[80]
	Glandular tissue	3.24 ± 0.61	
	Fibroadenoma	6.41 ± 2.86	
	IDC	10.40 ± 2.60	
	DCIS	15.62 ± 2.64	
	High invasive carcinoma	16.38 ± 1.55	
		42.52 ± 12.47	
Compression tests	Adipose tissue	0.69 ± 0.19–19.08 ± 4.99	[81]
	Glandular tissue	0.73 ± 0.18–16.99 ± 4.92	
	DCIS	5.25 ± 0.46–16.15 ± 4.24	
	IDC	13.82 ± 9.60–30.50 ± 11.46	

IDC: invasive ductal carcinoma; ILC: invasive luminal carcinoma; DCIS: ductal *in situ* carcinoma.

Table 6. Advantages vs disadvantages of biofabrication approaches for scaffold-based models.

	Advantages	Disadvantages
Freeze-drying	Ease process Porous interconnectivity	Heterogeneous porosity Influence of freezing
Particulate leaching	Macro-porosity Porous interconnectivity	Heterogeneous porosity
Cryo-polymerization	Simple, fast, low-cost method	Low temperatures Long time of preparation
3D printing	Homogeneous porosity Precise fibers alignment	High costs Post-printing crosslinking

of sample obtainment, while limitations regard the difficulty in controlling pore size and shape due to interplay between thermodynamics and kinetics. Temperature profiles (e.g. temperature reduction to final freezing) strictly affect the pore structure and size within the scaffold [75]: fast temperature decrease can lead to heterogeneous architecture, while slower and controlled freezing rate brings to a more homogeneous structure. Particulate leaching (figure 10(B)) is a technique which allows to obtain macro-porous scaffold-based models with a wide range of pore dimensions (30–300 μm), promoting an efficient infiltration of the cells and of the required nutriments [84]. Cryo-polymerization (figure 10(C)) represents a more recent approach of scaffold fabrication through a simple, fast, and low-cost method. Cryo-polymerization allows to obtain versatile platforms to investigate breast cancer behavior and to screen anticancer drugs [83]. Alternatively, 3D printing is the prominent AM technology which allows to print constructs in a layer-by-layer fashion, selecting precise biomaterials or biomaterials inks to fabricate constructs with physical and biological properties like those of breast cancer tissues [85] (figure 10(D)). Models are thus 3D printed and crosslinked to be stabilized or freeze-dried to generate interconnected pores. Then, cells are suspended in culture medium and cultured onto the surface.

2.3.2.1. State-of-the-art scaffold-based models and their evolution

The advent of 3D scaffold-based models allowed to increase the degree of complexity in breast cancer *in vitro* cells culture (table 7); as such, free drugs directly administered in conventional 2D cultures have been completely bypassed, and modern DDSs, coupled with 3D models, gained attention to develop innovative treatments. The importance of culturing breast cancer cells on a scaffold resides in the better mimicking of their potential antidrug resistance, which is enhanced in sustaining biomaterials with respect to standard TCPS culturing plates.

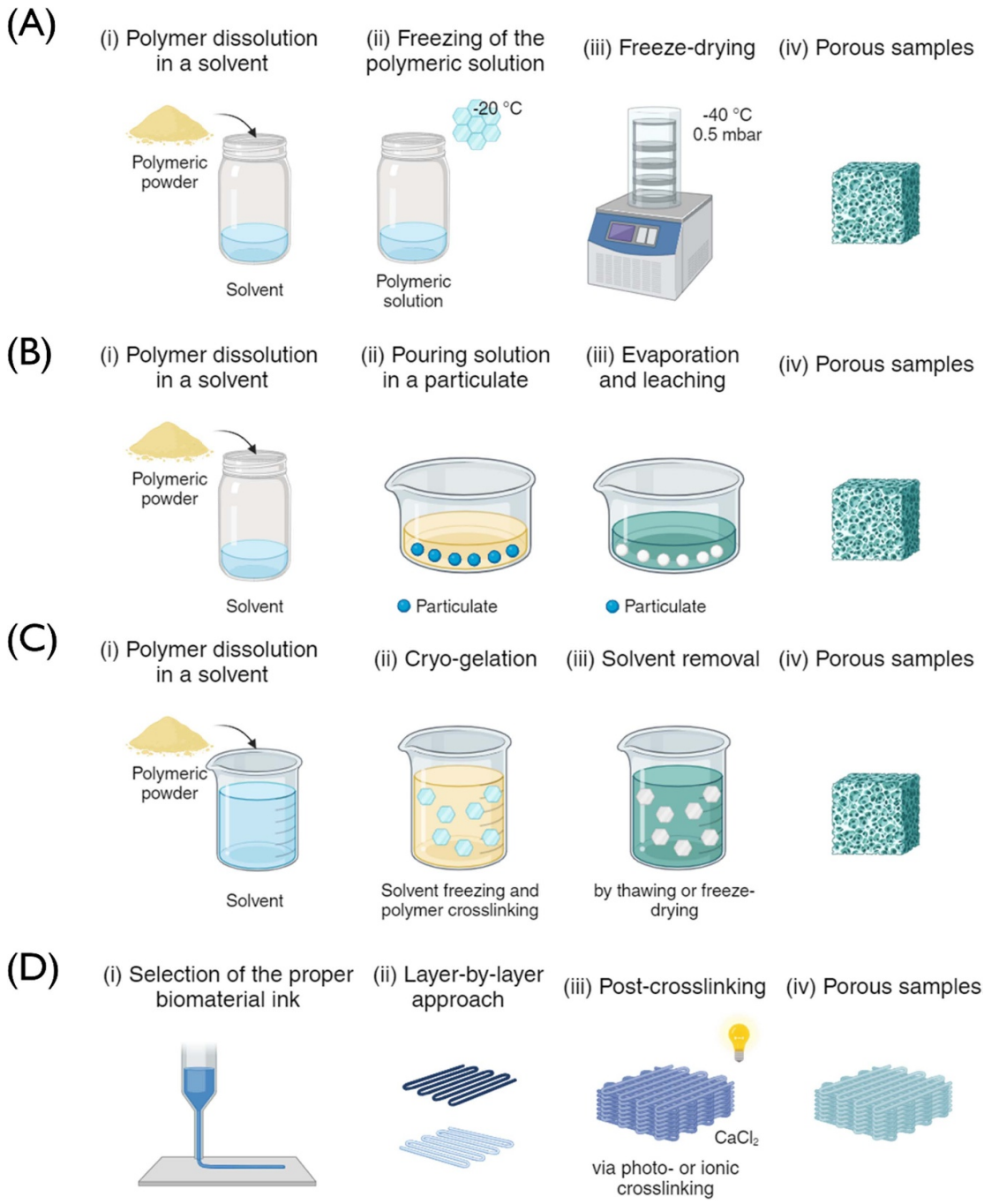

Figure 10. Technologies for scaffold-based models formation. (A) Freeze-drying. (B) Particulate leaching. (C) Cryo-polymerization (D) 3D printing. Created in BioRender. Pitton (2026) https://BioRender.com/nb60ve2. Created in BioRender. Pitton (2026) https://BioRender.com/ppoxwkf. Created in BioRender. Pitton (2026) https://BioRender.com/9anuepv. Created in BioRender. Pitton (2026) https://BioRender.com/j06sycv.

Cell response to drug administration is thus more similar to the *in vivo* response. Currently, natural products, as herbal medicine, are widely investigated as a novel and complementary treatment for anticancer therapies. For example, geniposide (GEN) has been studied by Lv *et al*, due to its reported advantages in alleviating clinical symptoms and prolonging cancer patient survival. This natural compound has been demonstrated to be able to induce breast cancer cells apoptosis and differentiation, strengthening the immune system and inhibiting angiogenesis. GEN has been confirmed to inhibit MCF7 breast cancer cells growth when seeded onto 3D printed (and subsequent freeze-dried) gelatin/chondroitin sulphate scaffold-based models, up to 72 h of cell culture. The effect of GEN was dose-dependent, as by constantly increasing concentration of the natural drug, the number of living cells on the scaffold surface gradually decreased [82]. Alternatively, curcumin is arising as a novel therapeutic agent to inhibit breast cancer proliferation. Su *et al* have developed nanoparticles, based on Pluronic F127, which delivered curcumin

Table 7. Scaffold-based 3D *in vitro* models for breast cancer mimicry.

Fabrication	Dimensions and cell density	Materials	Cells	Application	Results	References
3D printing, EDC/NHS crosslinking, freeze-drying	$V = 5 \times 5 \times 2$ mm^3 Den $= 1 \times 10^7$ cells ml^{-1}	CS Gel	MCF7	Investigating the GEN inhibition on breast cancer cells	CS/Gel scaffolds with good biocompatibility Cell survival ↓ after 48 h of GEN exposure	[82]
3D printing, $CaCl_2$ crosslinking, EDC/NHS crosslinking, freeze-drying	$D = 10$ mm $h = 5$ mm Den $= 2 \times 10^5$ cells scaffold^{-1}	Pluronic F127 Gel Alg NC	MDA-MB-231 L929	Investigating curcumin-loaded NPs effects on proliferation of breast cancer cells	Curcumin-loaded NPs ↓ cell viability Anticancer effect ↑ than 2D culture	[85]
EDAC/NHS crosslinking, freeze-drying	$D = 9$ mm $h = 4.5$ mm Den $= 1 \times 10^5$ cells scaffold^{-1}	Col Gel	MCF7	Evaluating scaffold ability to support attachment, infiltration, and proliferation of breast cancer cells	Homogeneous and ↑ porosity Col scaffolds exhibited 1.2 kPa stiffness (+EDAC) Gel addition ↑ scaffolds stiffness (1.3–1.7 kPa) MCF7 viability (90%)	[86]
3D printing, freeze-drying	$V = 30 \times 30 \times 5$ mm^3 Den $= 3 \times 10^5$ cells scaffold^{-1}	TEMPO-NCFs	MCF7 MDA-MB-231	Investigating a promising 3D scaffold-based platform for drug screening	Pores size ∼ hundreds of μm 3D models ↑ marker CD44 and migration marker VIM	[87]

(Continued.)

Table 7. (Continued.)

Fabrication	Dimensions and cell density	Materials	Cells	Application	Results	References
Cryo-polymerization	$V = 4 \times 4 \times 1$ mm^3 Den $= 3 \times 10^6$ cells ml^{-1}	Hyaluronic acid	NIH/4T1	Evaluating the impact of biochemical cues of hyaluronic acid-based cryogels on CD44$^+$ cells	Large (75 μm) and interconnected pores (>80%) 4T1 attached to RGD-scaffold 4T1 ↑ cell–cell interactions in RGD-scaffold	[83]
3D printing, $CaCl_2$ crosslinking	$D = 20$ mm $h = 2$ mm Den $= 1 \times 10^6$ cells scaffold^{-1}	Alg Periostin Hydroxyapatite	MCF7 MDA-MB-231	Investigating 3D breast cancer model as anticancer drugs platform screening	Cells clustered in 3D ↑ expression of CD44 and TWIST1 ↓ expression of proliferative markers MKI67	[88]
Particulate leaching	$V = 10 \times 10 \times 8$ mm Den $= 2 \times 10^5$ cells scaffold^{-1}	P(3HO-co-3HD) P(3HB)	MCF7 MDA-MB-231	Resembling TME and gene expression	Pore size ranging 30–300 μm MDA-MB-231 grew in clusters MCF7 grew in a dense layer	[84]

V: volume; Den: cellular density; CS: chitosan; Gel: gelatin; MCF7: human breast cancer cells; GEN: geniposide; D: diameter; h: height; Alg: alginate; NC: nanoclay; MDA-MB-231: human metastatic breast cancer cells; L929: murine fibroblasts; NPs: nanoparticles; Col: collagen; NCFs: cellulose nanofibrils; NIH/4T1: murine breast cancer cells; P(3HO-co-3HD), P(3HB): PHAs biomaterials, synthesized by microorganisms; TME: tumor microenvironment; EMT: epithelial-to-mesenchymal transition.

to MDA-MB-231 breast cancer cells seeded on scaffolds made of 3D printed gelatin/alginate/nanoclay. These models have been printed and subsequently crosslinked with $CaCl_2$ immersion and EDC/NHS and finally freeze-dried. Findings enlightened how curcumin-loaded nanoparticles critically diminished cell viability of seeded breast cancer cells, making promising the investigated nanomedicine approach to delivery anticancer drugs [85].

Collagen-based scaffold models have been largely exploited for breast cancer research, due to their similarity with the composition of the breast ECM, which is rich in collagen. Redmond *et al* developed collagen-based scaffolds that support attachment and proliferation of MCF7 breast cancer cells in a 3D matrix. Freeze drying allowed the obtainment of highly porous (>99%) scaffolds with homogeneous (150–300 μm) and interconnected pores. The main issue of matching mechanical properties of breast cancer tissues was achieved by strengthening collagenous scaffolds through EDAC crosslinking, which enhanced stiffness to 1–2 kPa, resembling cancerous breast tissue. Moreover, the addition of gelatin into the scaffold allowed the tuning of its porosity and pore size, of its stiffness (1.3–1.7 kPa), and also increased MCF7 viability and proliferation [86]. The manipulation of gene expression profiles of breast cancer cells resulted to be strictly depending on the surrounding matrix and growth conditions. Rosendahl *et al* printed TEMPO-cellulose nanofibers (CNFs) constructs to investigate different breast cancer cell lines (MCF7, MDA-MB-231) behavior, aiming to obtain a drug screening platform. The genes induction from 3D ECM, associated with stemness, migration, pluripotency, differentiation, and proliferation, in cells cultured onto TEMPO-CNFs printed scaffolds were analyzed and compared to standard 2D conditions. Findings showed that the surrounding matrix induced the expression of marker $CD44^+$ and migration marker VIM in both cell lines [87].

A novel method to fabricate scaffolds requires cryo-polymerization. Cryogels were optimized by Rezaeeyazdi *et al*, by employing HA as a promising platform to culture breast cancer cells. Referring to the crucial role of HA in breast ECM, cryogels aimed to investigate interactions between the engineered ECM and $CD44^+$ breast tumor cells NIH/4T1. Findings enlightened that a monolayer of tumor cells had developed in RGD-modified cryogels, whereas cells cultured onto RGD-free cryogels have resulted in a large and dense growth of micro-tumor-like formations, which appeared more similar to the *in vivo* tumor mass [83]: the importance of providing cells with an engineered matrix resulted crucial to obtain a response like the *in vivo* behavior. Non-adherent hydrogels to obtain 3D models were also investigated by Svanstroom *et al*, who fabricated non-adherent alginate hydrogels for breast cancer. Key properties of alginate reside in its tunable properties and chemical inertia. As HA, alginate can be functionalized to obtain stable hydrogels whose physical and mechanical properties can be consequently tailored to trigger a proper biological response from cells seeded onto its surface. In this case, stiffness was increased with the addition of hydroxyapatite deposits, to resemble micro-calcification typical of breast cancer; in addition, periostin, overexpressed in breast cancer, was used as an additive. Alginate concentration turned out to be a key parameter to determine cell viability. Increased expression of $CD44^+$ and EMT transition markers (TWIST1) was observed, whereas proliferation markers (MKI67) decreased [88].

An innovative solution to build scaffold-based 3D models refers to the involvement of polyhydroxyalkanoates (PHAs). Tomar *et al* used PHAs to build scaffolds with suitable shapes and dimensions, adequate interconnected pores, and adequate mechanical properties to mimic breast cancer ECM. As such, porous scaffolds have been generated with variable pore size, allowing infiltration of cells and passages of nutrients, oxygen, and metabolites. Remarks enlightened the invasive capability of MDA-MB-231 cells instead of less aggressive phenotype expressed by MCF7 cells [84].

The interest related to scaffold-based models for breast cancer progressively diminished due to the emergent technologies of hydrogels and bioprinted models. Porous scaffolds guaranteed a 3D sustaining biomaterial which ensured to respond to the clinical need which required the presence of an external and surrounding ECM for cancer study. Additionally, pore presence allowed the flow exchange of culture medium, oxygen and waste products internally and externally to the hydrogel. However, emergent drawbacks, related to their poor controllability and the impossibility to directly incorporate cells into the biomaterial, progressively limited the involvement of porous scaffolds in breast cancer modeling.

2.3.3. Hydrogel-based models

Hydrogels-based constructs have been developed to build breast cancer *in vitro* models due to their great potential in tissues mimicry and their promising features, such as biocompatibility and biodegradability, large water content, low inflammatory activity, suitable/tunable physical and mechanical properties, and, moreover, possibility to encapsulate cells. In fact, the possibility to finely tailor hydrogels properties and to directly embed cells represents the main advantage in using these materials for breast tumor modeling with respect to scaffolds [72]. Of course, their features strictly depend on the selected biomaterial and on its degree of crosslinking: a higher crosslinking ratio results in lower water uptake, lower degradation kinetic, and, consequently, higher mechanical properties; contrarily, a higher water absorption and poor

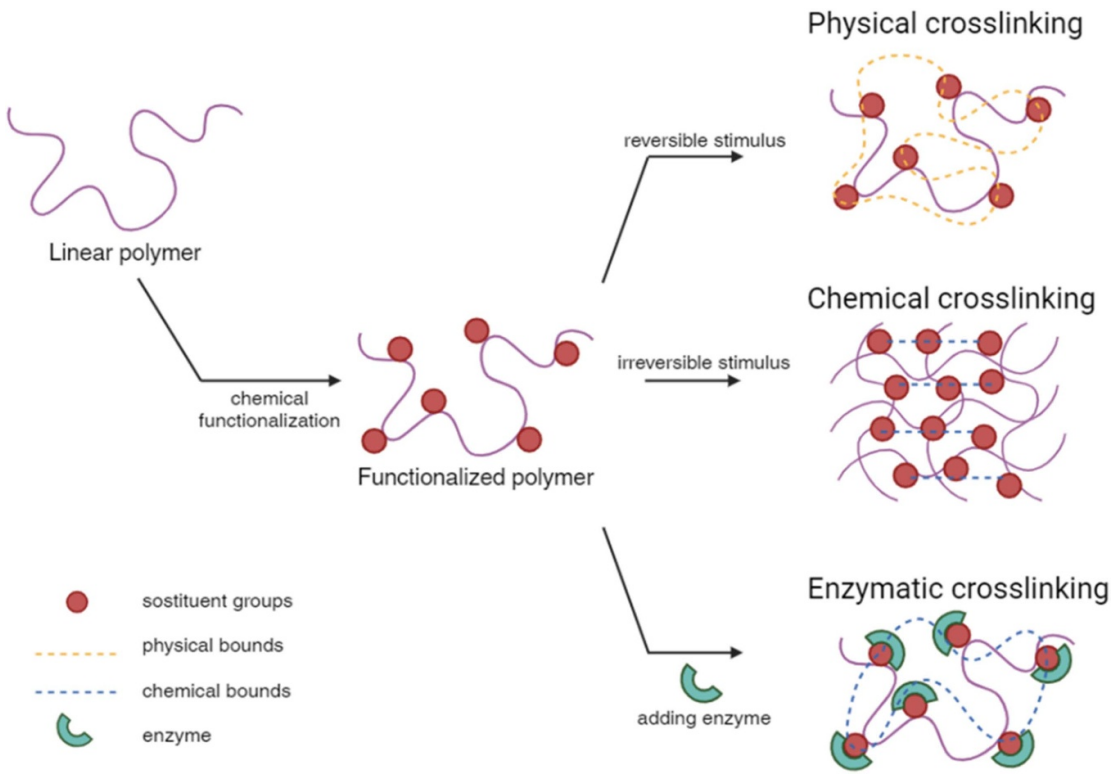

Figure 11. Approaches for hydrogel-based models obtainment: physical crosslinking (upper) which confers reversible bonds; chemical crosslinking (intermediate) which generates irreversible covalent bonds; enzymatic crosslinking (lower) which forms irreversible covalent bonds towards the addition of a chemical enzyme. Created in BioRender. Pitton (2026) https://BioRender.com/ry16f32.

mechanical properties are associated with low crosslinked structures.

Natural hydrogels require crosslinking to confer adequate mechanical stability to their structure. Crosslinking methods can be distinguished in physical, chemical, and enzymatic approaches (figure 11). Physical crosslinking can be established in thermoresponsive polymers, which behave as gel above or below defined transition temperatures. Chemical crosslinking allows covalent or ionic bonds to be introduced among precise chemical residues in polymeric backbones. Among possible chemical crosslinking approaches, bivalent ions or photocrosslinking are the most widely investigated methods [9]. Negatively charged polysaccharides like alginate or pectin can be ionically crosslinked by reaction with bivalent ions of $CaCl_2$ (Ca^{++}), forming typical *egg-box* structures which confer stability to the polymeric network. Furthermore, chemical functionalization of natural biomaterials allows the addition along their polymeric backbone of light-sensitive motifs, which can form stable covalent bonds among polymeric chains after light exposure. Alternatively, enzymatic crosslinking requires the addition of a proper enzyme to successfully introduce crosslinks into various protein matrices. For example, transglutaminases are one of the most employed families of photo-reaction initiators. Alternatively to conventional crosslinking reactions, cell-laden hydrogels can be built through *click chemistry* reactions or *self-assembling peptides*, which represent an alternative crosslinking strategy with improved ease-of-use [89]. Click chemistry process requires only two hydrogel precursors, omitting the need for external stimuli (e.g. light source or photoinitiators), exploiting reactions which are *as simple as the clicking of interlocking fasteners* to form endless numbers of linkage chemical bonds [87]. By combining residual groups along the polymeric backbone, crosslinking can be triggered with the consequent formation of stable hydrogels. Regarding self-assembling peptides, these hydrogels recently emerged as suitable platforms for tumor modeling due to their possibility to adjust mechanical and biochemical properties. Advantages in the use of this unconventional method refers to the mild conditions of the reaction and its short time process; minimum byproducts are produced, and easy purification is required; however, there is a strict control of the process parameters to successfully obtain stable hydrogels [89].

Due to their high biocompatibility, biological cues, and tunable features, natural biomaterials have been widely employed to form hydrogels: collagen, gelatin, GelMA, HA, alginate and dECM. Collagen-based hydrogels can be fabricated by tailoring their pores size and stiffness, to manipulate cell alignment, progression, and invasion. Gelatin requires crosslinking to generate stable and mechanically relevant

hydrogels. Hence, gelatin polymeric backbone can be decorated with light-sensitive methacryloyl groups, forming GelMA, able to form covalent bonds when exposed to light with a specific photoinitiator. GelMA has gained particular interest in biomedical research due to its photosensitivity, since physical and mechanical features can be finely tailored to mimic breast cancer ECM. HA found wide application due to its binding points for CD44 gene, expressed by tumor cells, which are targeted sites for breast cancer cells to promote their proliferation and metastatic behavior. Among polysaccharides, alginate has been then investigated for its easy and biocompatible crosslinking of bivalent cations, allowing for spatial crosslinking. Culture of breast cancer cells in non-adhesive alginate hydrogels results in the formation of typical cancer-like clusters, whose size represents their response to anticancer treatments [90]. To provide cells an adequate matrix which resembles the proteinaceous components of breast ECM, dECM has been also investigated. Contrarily, synthetic hydrogels allow to increase reproducibility of hydrogels features, even though they lack biomolecular cues present in natural hydrogels (e.g. PEG, poly(Nε-acryloyl L-lysine) hydrogels) which can enhance cell response.

2.3.3.1. State-of-the-art hydrogel-based models and their evolution

One of the main advantages in using hydrogels resides in the possibility to directly encapsulate one or more types of cells, either healthy or tumoral, into the polymeric structure, which can be also modified and enriched with bioactive molecules, e.g. cell-adhesive peptides, enzyme-sensitive peptides, and growth factors binding [9]. Crosslinking methods, biomaterials, and cells involved in fabricating hydrogel-based breast cancer models have been reported in table 8.

Collagenous hydrogels have been largely investigated to understand how microenvironmental cues influence the angiogenic response of cancer cells with the secretion of VEGFs. It has been reported that an ECM-derived mechano-transduction pathway seems to trigger angiogenesis from tumor cells [91]. Nasser *et al* investigated if the interruption of this signaling could stand out as a potential novel therapy against breast cancer progression, disrupting tumor vascularization, and repressing tumor growth. Collagenous hydrogels were fabricated starting from a non-enzymatic pre-glycation of collagen, known as Maillard reaction, with the encapsulation of MDA-MB-231 breast cancer cells prior to gel formation. Results showed that the cell-laden hydrogels exhibited an increase in the production of pro-angiogenic factors; the inhibition of mechano-transduction pathway Rho/ROCK via Y-27632 diminished cellular angiogenic potential [91].

Combination of gelatin and alginate has been extensively investigated in literature [73, 92, 93] due to the advantages provided by both biomaterials: gelatin as collagen-derivative and due to the presence of RGD motifs, and alginate due to its ease crosslinking. Physical and chemical properties of cell-laden hydrogels, such as stiffness, matrix composition, pH and interstitial fluids, known to be dysregulated in tumor progression, cause different responses in different types of breast cancer cells. Shah *et al* fabricated gelatin/alginate hydrogels, in which they encapsulated MDA-MB-231 and MCF7 cells, by varying ECM stiffness, ranging from 2 to 10 kPa (i.e. malignant condition), and also pH values: pH values equal to 6.5–6.9 have been associated to angiogenesis, tumor aggressiveness and disruption of cellular circadian clock [92]. In addition, the same gelatin/alginate combination has been employed to generate metastatic tumor 3D models to study invasiveness of breast cancer cells. A proper combination of gelatin/alginate was engineered to mimic the stiffness of healthy (1–2 kPa), and cancerous (6–10 kPa) breast tissues. Encapsulated MDA-MB-231 metastatic breast cancer cells migrated faster in stiffer hydrogels (>6 kPa), while they showed a decrease in motion in softer hydrogels (<3 kPa): stiffness of the matrix thus affects cell migration ability [92]. De Dios-Figueroa *et al* also employed and characterized gelatin/alginate hydrogels to build breast cancer models for preclinical screening for new therapeutics. Encapsulated BT-474 breast cancer cells remained highly viable (>90%) up to 10 d of culture, and expressed HER2 targeting factors, which can be potentially used for cancer therapy [93]. Alternatively, dECM allows to realize hydrogels characterized by preserved ECM components and original structure. Xu *et al* co-cultured L929 fibroblasts and 4T1 murine breast cancer cells to develop screening platforms for anticancer drugs investigation. dECM from fresh porcine liver was enriched with the addition of gelatin, to increase hydrophilicity and viscoelasticity, and alginate, to enhance structural mechanical properties, making them comparable to those of breast cancer tissues (9.64 kPa). 4T1 cells exhibited high viability and spheroid-like structures (150 μm) in dECM/gelatin/alginate hydrogels [73].

Lastly, alginate has also been used for breast tumor ECM mimicking, by exploiting its advantages of easy handling and crosslinking, enabling the formation of complex structures. Hence, Barros da Silva *et al* developed a model of breast cancer matrix by fabricating a RGD-modified alginate model with embedded CAFs. The pores of the obtained structure were filled with a MCF10A-laden oxidized peptide-modified alginate hydrogel to build the parenchymal compartment. Results enlightened how the hydrogel sustained epithelial morphogenesis if surrounded by fibroblasts and ECM, whereas proteome profiling of digested hydrogel exhibited upregulation of proteins associated with aggressive phenotypes of MCF10A (e.g. matrix assembly/remodeling, EMT, cancer) [94].

Table 8. Hydrogel-based 3D *in vitro* models for breast cancer mimicry.

Fabrication	Dimensions and cell density	Materials	Cells	Application	Results	References
Maillard reaction	Den = 12.5×10^4 cells gel^{-1}	Col	MDA-MB-231	Investigating matrix-associated tumor angiogenesis and screening therapeutic agents	↑ pro-angiogenesis factors ROCK ↓ pro-angiogenesis signaling	[91]
Crosslinking via 0.1 mM $CaCl_2$	Den = 2×10^6 cells ml^{-1}	Alg Gel	MDA-MB-231	Developing breast-to-bone metastasis (bone mimicking towards PCL scaffolds)	Elastic modulus 1.8–10.1 by ↑ Gel ↑ expression of osteolytic factors PTHrP and IL-6 if MDA-MB-231 are in stiffer hydrogels	[92]
Crosslinking via 0.1 mM $CaCl_2$	$D = 7$ mm $h = 7$ mm Den = 2×10^6 cells ml^{-1}	Gel Alg	MCF7 MDA-MB-231	Studying interplay between cancer cells and engineered ECM	Stiff and dense hydrogels (10 kPa) and acidic pH (6.5) play key role in MCF7 sensitiveness Cells aggregate ↑ in dynamic conditions	[21]
Crosslinking with 150 mM $CaCl_2$	Den = 5×10^5 cells scaffold^{-1}	Gel Alg	BT474/GFP	Charactering hydrogels to mimic 3D breast cancer behavior	Pore size ranging 20–125 μm 90% viability up to 10 d Expression of HER2 for anticancer therapies	[93]
Crosslinking via 3% $CaCl_2$ and EDC/NHS	$A = 5 \times 5$ mm^2 $h = 1$ mm Den = 1×10^6 cells ml^{-1}	dECM Gel Alg	L929 4T1	Investigating an effective platform for anticancer drug screening	Gel ↑ viscoelasticity Alg ↑ mechanical properties and porosity Elastic modulus = 9.64 kPa Spheroids formation ($D = 150$ μm)	[73]
Pouring of cell-laden Alg-based hydrogels in printed constructs	Den = 2–5 $\times 10^6$ cells ml^{-1}	Alg-RGD (3D printed) oxALG-RGD-PVGLIG (with cells)	MCF10A CAFs	Developing a hybrid 3D model with epithelial and CAFs cells and ECM	Cell-laden Alg hydrogels formed parenchymal compartment Hydrogels supported epithelial morphogenesis Upregulation of proteins associated with matrix remodeling, EMT and cancer	[94]

(Continued.)

Table 8. (Continued.)

Click Chemistry	Den $= 1 \times 10^6$ cells ml^{-1}	ELR	MCF7 MDA-MB-231 MCF10A	Investigating the ELRs suitability in mimicking ECM breast tumor	MDA-MB-231 formed cell networks Expression of ECM High drug resistance	[95]
Self-assembling peptides	Den $= 1 \times 10^6$ cells ml^{-1}	PeptiGel®Alpha1	MCF7 MDA-MB-231	Self-peptides hydrogels to mimic 3D breast cancer behavior	Peptides recapitulate hypoxia and invasion MCF7 forming large clusters resembling breast acini MDA-MB-231 remaining dispersed	[96]
Self-assembling peptides	Den $= 1 \times 10^6$ cells ml^{-1}	$(FFiK)_2$	MCF7	Self-peptides hydrogels to mimic 3D breast cancer behavior	High cell viability Proliferation forming clusters when expressed RGD and PHSRN AG73 markers ↑ invasion capability	[97]
Self-assembling peptides	Den $= 0.5 \times 10^5$ cells ml^{-1}	PeptiGel® Alpha4 Laminin	CSCs	Self-peptides hydrogels to mimic 3D breast cancer behavior	Laminin addition to PeptiGel® ↑ signals for reaching matrix polarization and expression of proteins	[98]

Den: cellular density; Col: collagen; MDA-MB-231: human metastatic breast cancer cells; Alg: alginate; Gel: gelatin; PCL: polycaprolactone; D: diameter; h: height; MCF7: human breast cancer cells; ECM: extracellular matrix; BT474: breast cancer cells; A: area; dECM: decellularized extracellular matrix; L929: murine fibroblasts; 4T1: murine breast cancer cells; D: diameter; ELR: elastin-like recombinamer; MCF10A: human normal breast cells.

Click chemistry reaction was carried out by Blanco-Fernandez *et al* to build hydrogels fast and in mild conditions. Elastin-like recombinamer (ELR) hydrogels were formed by click chemistry reaction of two ELR polypeptides, one containing sequences for biodegradability and the other carrying groups for cell adhesion [95]. These polypeptides crosslink above certain temperatures thanks to hydrophobic interactions. Encapsulated breast cancer (MCF7, MDA-MB-231) or non-tumorigenic (MCF10A) cells showed high viability and proliferation up to 7 d of culture. In particular, MCF7 and MCF10A formed spheroids, whereas MDA-MB-231 established cell networks [95]. Alternatively, self-assembling peptides have been involved in the modeling of breast cancer ECM, since molecular assembly has recently gained particular attention for hydrogels developing. Self-assembled hydrogels offer an advantageous well-defined chemical structure, diminishing batch-to-batch variability which drastically affects the reproducibility of natural hydrogels. Clough *et al* compared self-assembled hydrogels from PeptiGel®Alpha1 with collagen hydrogels; both the formulations were encapsulated with MDA-MB-231 and MCF7 breast cancer cells. Results enlightened the promising applicability of PeptiGel®Alpha1 hydrogels, as breast cancer cells showed similar behavior of those encapsulated in collagen hydrogels: MCF7 cells formed large aggregates with great number of cells up to day 14 of culture, while MDA-MB-231 cells resulted in loose aggregates of irregular shape, reflecting their invasiveness [96]. Moreover, other self-assembling peptides have been employed by Chia *et al*, who used short self-assembling peptides $(FFiK)_2$ with a symmetric structure connected with urea bonds. These hydrogels were functionalized with bioactive sequences to promote cancer cells growth: RGD/PHSRN derived from fibronectin and AG73/C16 from laminin. Results enlightened how encapsulated MCF7 cells proliferate forming clusters when RGD and PHSRN sequences are expressed, while their invasiveness is enhanced with laminin-derived sequences [97]. More recently, Lingard *et al* tried to limit batch-to-batch variability of hydrogels by using self-assembling PeptiGel® to model breast *in vitro* ECM for mammary epithelial cells. They proved the self-assembling hydrogels could sustain the viability of encapsulated cells, but cell proliferation was significantly enhanced by adding laminin to the model and consequently adjusting the stiffness of the supporting matrix. Moreover, the increased stiffness ensured changes in protein expression associated with altered function of the TME [98].

Contrarily to scaffold-based models, hydrogels ensured the faithful mimesis of the mechanical features for breast tissues. Their main advantages regard the tuneability of their properties, which could be finely adjusted to allow the mimicking of the desired stiffness or recovery ability, and the possibility to directly embed cells in a sustaining matrix. To date, hydrogels have gained huge interest due to the possibility to fully answer the requests from oncology research, aiming to develop platforms where cells could exploit their drug or therapies resistance compatible with their *in vivo* response.

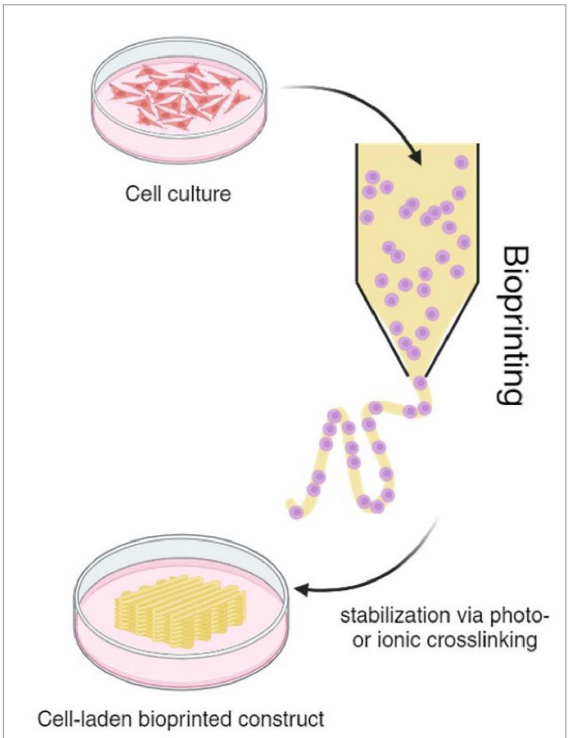

Figure 12. Bioprinting process. Cells are expanded in 2D cell cultures and mixed in biomaterial inks (bioinks). Bioinks are then dispensed layer-by-layer in 3D cell-laden models which are stabilized towards photo- or ionic crosslinking. Created in BioRender. Pitton (2025) https://BioRender.com/iuvm7iv.

2.3.4. Bioprinted models

3D bioprinting has recently gained attention in the development of tumor models with precise control over breast cancer cells (and eventually stromal cells) arrangement (figure 12). Moreover, in the last years, improvements have made it possible to print different bioinks with different conformations, increasing the degree of complexity of 3D bioprinted models with high spatial accuracy.

The main advantage of bioprinting is associated with its great scalability and with the achievable complexity degree of the resulting constructs, which is crucial for recreating the breast TME complexity and its functional and structural hierarchies, for an accurate study of tumor growth, treatments response, and other biological features of cancer biology [99]. High complexity allows the possibility of introducing tumor models to develop personalized treatments plans or evaluation of anticancer drugs. 3D bioprinting technology includes extrusion-based bioprinting, inkjet bioprinting, laser assisted printing, and

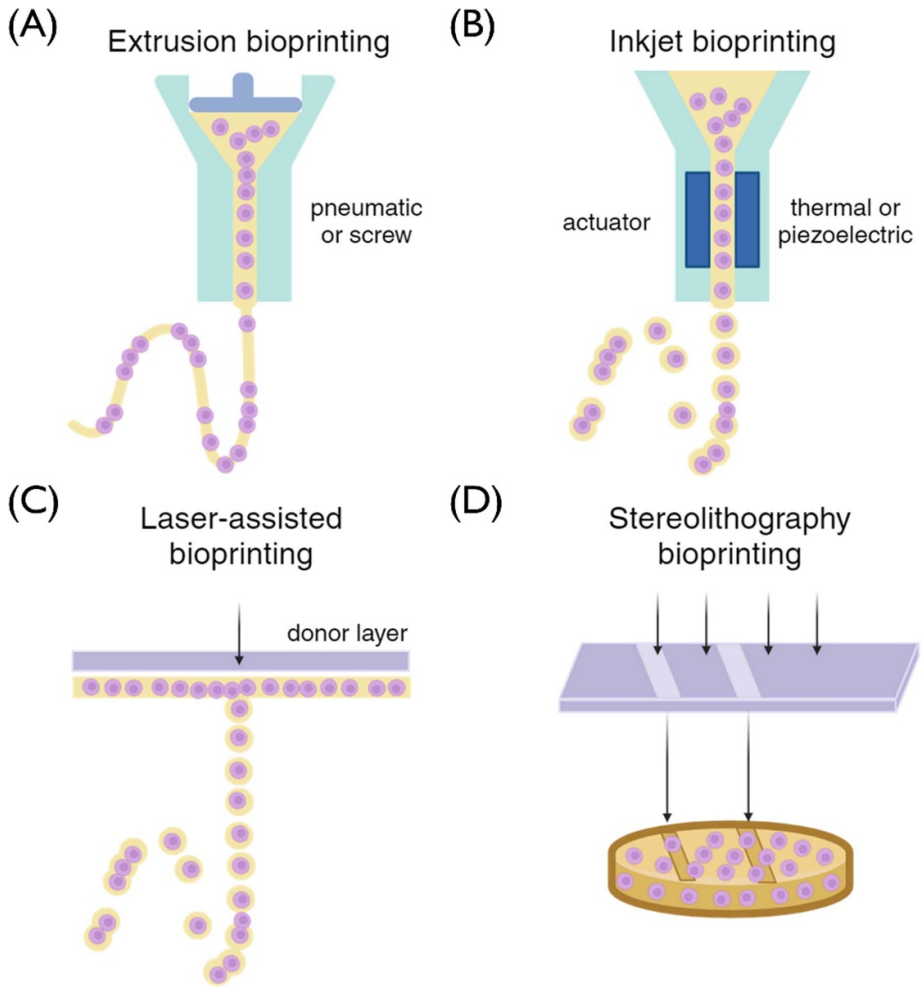

Figure 13. Technologies for 3D bioprinted models formation. (A) Extrusion bioprinting. (B) Inkjet bioprinting. (C) Laser-assisted bioprinting. (D) Stereolithography bioprinting. (A), (B) Created in BioRender. Pitton (2026) https://BioRender.com/43sztp7. (C), (D) Created in BioRender. Pitton (2026) https://BioRender.com/75ecnbq.

stereolithography (figure 13); however, extrusion-based bioprinting results the most common method due to its simplicity and lower costs with respect to the other printing approaches [73]. Bioinks must exhibit essential properties to allow the process of extrusion-based 3D bioprinting: printability during the process and accurate shape fidelity after the printing (shear-thinning behavior); mechanical properties suitable for cell adhesion, proliferation and differentiation. The major challenge with adapting these materials for bioprinting thus lies in balancing chemical, mechanical, rheological, and biological properties in order to develop bioinks which are mechanically stable, printable, and biocompatible. Most of the traditional biomaterials, e.g. collagen, gelatin, alginate, dECM, used for 3D cell culture, lack of the required rheological properties for extrusion-based printing, and must be modified to meet the bioprinting demands [100]. Moreover, bioprinted constructs often require proper post-crosslinking to confer mechanical stability. Other advantages are associated with the possibility of controlling the process through computer programs that design the model in specific software and adjust the printing parameters to best suit the obtainment of the desired constructs. Specifically, printing parameters can be set and modified in real-time during the process of printing. Bioprinted models thus result in high reproducibility, high throughput, and high efficacy [73]. Enhancing mechanical properties and stability of bioprinted constructs can be achieved by adding secondary polymers incorporation, utilizing supramolecular hydrogels, forming nanocomposites [100].

2.3.4.1. State-of-the-art bioprinted models and their evolution

Applications for 3D bioprinted models, with the used bioinks and cells, are reported in table 9. One of the main advantages of 3D bioprinting is the possibility to print cells and biomaterials in a breast cancer tumor-inspired manner: for this purpose, bioprinted models often comprise a central core made of tumor cells, surrounded by a stromal cell compartment, closely mirroring the breast tumor niche. Blanco-Fernandez *et al* used dECM from breast tissues to obtain a bioink with a natural-derived proteinaceous component and

Table 9. Bioprinted 3D *in vitro* models for breast cancer mimicry.

Fabrication	Dimensions and cell density	Materials	Cells	Application	Results	References
Photocrosslinking with UV, chemical crosslinking with $CaCl_2$	$D = 3$ mm $h = 1.02$ mm Den $= 1 \times 10^6$ cells ml^{-1} (hAMSC) Den $= 1.5 \times 10^6$ cells ml^{-1} (hAMSC)	TDM GelMA + I2959 Alg Col	MCF7 hAMSC	Investigation of printability of TDM breast hydrogels for breast cancer mimicry	GelMA and Alg addition in TDM ↑ printability, shape fidelity and cytocompatibility Col ↑ printability and mimicry ↓ expression of E-cadherin in cell aggregates Downregulation of HSP90 DOX sensitivity and ↑ breast cancer proliferation	[105]
Photocrosslinking with UV	$D = 2.5$ mm $h = 1$ mm $V = 1 \times 1 \times 0.3$ cm (tumor stroma) Den $= 1 \times 10^7$ cells ml^{-1} (MDA-MB-231)	dECM MeHa + I2959	MDA-MB-231 MCF7 HBF EC	3D printing to mimic native tumor ECM, study therapeutic effect and investigate tumor progression	MeHA addition ↑ shape fidelity and viscosity MDA-MB-231 expressed SLUG and TWIST1, promoting EMT, associated to CSC ↑ TGF-β1 → interplay between cancer and CAF	[101]
Chemical crosslinking with 0.05 M $CaCl_2$	Den $= 5 \times 10^5$ or 1×10^6 cells ml^{-1} (MDA-MB-231)	Alg Gel	MCF7 ADSC	Multicellular and multicomponent bioink to model tumor microenvironment	Viability up to 10 d Significant lipid presence in hydrogel co-culture Lipids appeared more clustered	[102]
Chemical crosslinking with 200 mM $CaCl_2$	$D = 2.5$–5 mm $h = 0.5$–1 mm Den $= 1 \times 10^7$ cells ml^{-1}	Alg Gel	ZR75.1	Multicomponent bioink to screen *in vitro* drugs comparing to animal models	Cells proliferated in the bioink Similarities with tissues sections in cell morphology (e.g. luminal structures) ↑ sensitivity to *in vivo* animals	[103]

(Continued.)

Table 9. (Continued.)

Photocrosslinking	Den = 1×10^6 cells ml^{-1}	GelMA + LAP LPN-RD	MCF7	Developing a bioink for extrusion-based bioprinting for *in vitro* breast cancer	Shear thinning and viscoelastic behavior High viability of MCF7	[100]
Pepdite-induced crosslinking	Den = 3×10^6 cells ml^{-1}	Hyaluronic acid Protease degradable peptide (VPM-AZ_2) Non degradable PEG-bis-azide	hDF MCF7	Understanding protease role in tumor progression, cell proliferation, migration, and spheroids formation	MCF7 proliferation in protease degradable hydrogels (with fibroblasts) Limited proliferation in PEG based hyaluronic acid (with fibroblasts)	[52]
Crosslinking with 100 mM $CaCl_2$ (ALG and ALG-GEL) PEGDA-induced crosslinking (HA-SH)	Den = 1×10^6 cells ml^{-1}	Alg ADA-Gel HA-SH/PEGDA	MDA-MB-231 MCF7	Investigating tumor heterogeneity in different combinations of bioinks	Alg (3%) $\rightarrow$ highest stiffness ADA-Gel (2.5%) $\rightarrow$ softest Alg $\uparrow$ proliferation of breast cancer cells vs melanoma Alg, metabolism $\downarrow$ ALG1 and ADA-GEL2.5 $\rightarrow$ spheroids (80–100 μm) Mammary-gland structures up to 14 d (MCF7 cells)	[104]
HA-modification with pNIPAM (thermoresponsive)	$D = 8$ mm $h = 1.5$ mm Den = 1×10^5 cells ml^{-1}	Col Hyaluronic acid SF	21PT MDA-MB-231 HUVEC	Evaluating interactions between matrix components and breast tumor cells/CAFs phenotype	$\uparrow$ printability of Col in SF 21PT formed acinar colonies in Col/hyaluronic acid, while isolated colonies in Col gels	[106]
Tumor–stroma modeling by exposure at 37 °C for dECM crosslinking	1 cm × 1 cm × 3 mm (length, width, height) Den = 2×107 cells ml^{-1}	dECM	MCF7 MDA-MB-231 (core) HBF and THP-1 (stroma)	Investigating the potentiality of CSC-targeted therapy with a tumor–stroma model	Presence of biological signatures of dECM allowed a better response of CSC-targeted cells	[99]

D: diameter; h: height; Den: cellular density; TDM: porcine breast tissue; I2959: Irgacure; GelMA: methacrylate gelatin; Alg: alginate; Col: collagen; MCF7: human breast cancer cells; hAMSC: human adipose-derived mesenchymal stem cells; DOX: doxorubicin; V: volume; dECM: decellularized extracellular matrix; MeHa: methacrylate hyaluronic acid; MDA-MB-231: human metastatic breast cancer cells; HBF: stromal breast fibroblasts; EC: endothelial cells; ECM: extracellular matrix; ADSCs: adipose-derived stem cells; ZR75.1: luminal breast cancer cells; LPN: laponite; hDF: human dermal fibroblasts; ADA: alginate dialdehyde crosslinked; HA-SH: thiol-modified hyaluronan; SF: silk fibroin; 21PT: breast cancer cells; HUVEC: human umbilical vein endothelial cells; CAF: cancer-associated fibroblasts; CSCs:.

natural cues for biological interactions. However, dECM did not accurately resemble mechanical stability of targeted breast cancer ECM; consequently, this bioink was enriched with collagen, gelatin, and alginate to ensure good printability, appropriate elastic modulus and physical integrity. The core with MCF7 resembled the tumoral compartment, while the outer stromal portion was mimicked by human adipose-derived mesenchymal SCs (hAMSCs). Results showed typical tumoral pathways in MCF7 cells, such as lower expression of E-cadherin, and downregulation of HSP90, which reduced DOX sensitivity [95]. Bioprinted models characterized by an inner core and an outer layer have also been printed by Gonzalez-Callejo *et al*, aiming to study the reproduction of a tumor niche to investigate therapeutic treatments. dECM and methacrylate HA (HAMA) were combined, and different cell types were incorporated mimicking tumoral stroma (human breast fibroblasts, endothelial cells) or cancer mass (MDA-MB-231, MCF7). Incorporating different cells, the model expressed biomarkers associated with tumor biology: MDA-MB-231 expressed SLUG and TWIST1, which promote EMT, and high levels of TGF-β1, which is associated with interplays between cancer and CAFs [101]. Combinations of gelatin and alginate have been largely investigated as promising bioinks formulations, after alginate crosslinking in $CaCl_2$. Chaji *et al* demonstrated that a co-culture of MCF7 and ASCs cells exhibited a high viability up to 10 d of culture. Significant lipid deposition was evidenced in co-culture, and these droplets assumed a clustered morphology [102]. Then, Dankxó *et al* optimized the same gelatin/alginate combination, investigating the behavior of encapsulated and bioprinted ZR75.1. Cells proliferated in the bioprinted models, exhibiting similarities with tissue sections in terms of morphology. Moreover, in 3D bioprinted models, encapsulated cells showed a higher drug sensitivity if compared to *in vivo* studies [103]. Alternatively, GelMA was proven to be highly promising for obtaining 3D bioprinted breast cancer models, taking advantage from its photosensitivity and ease and biocompatible photocrosslinking process. Laponite was added to the bioink to increase its viscosity and elastic modulus (ranging from 0.2–75 kPa). MCF7 cells were encapsulated, demonstrating high cell viability in the bioprinted models [100]. Polysaccharides have also been employed to generate promising bioinks. For example, Boroojeni *et al* used HA, added with a protease-sensitive peptide (VPM-AZ_2) and a proper crosslinker (PEG-bis-azide) to understand the role of the protease in tumor progression, and cell proliferation, migration and spheroids formation. For instance, proteolytic degradation of ECM is essential for dynamic remodeling of the breast TME, and consequent dysregulation is crucial for disease progression. In cancer, protease, responsible for proteolytic ECM degradation, is secreted by cancer cells and CAFs. The investigation of protease-dependent hydrogels is useful to investigate dynamic crosstalk in cell-ECM interactions. Results enlightened an increase in cancer cells proliferation, especially in presence of co-cultured fibroblasts [52]. Alginate has been also used for resembling tumor heterogeneity in breast cancer models, taking advantage also from its prominent role in natural ECM and overexpression in cancer progression. Schmid *et al* have developed a library of different bioink formulations, made of pure alginate, ADA-alginate, HA-HS (crosslinked with PEGDA). It has been demonstrated that the stiffness of the bioink strictly affects the behavior of breast cancer cells, as well as the invasiveness capability of the breast cancer cell line [104].

Recently, multicomponent bioinks between collagen and polysaccharides (e.g. HA) have gained particular attention to enrich collagen bioinks to enforce the properties of the biomaterial. The addition of HA resulted in an increase in the printability of collagen bioink; moreover, 21PT cells tended to form acinar colonies, similar to the *in vivo* aggregates, in collagen gels [106]. Lately, improvements have been demonstrated by Gonzalez-Callejo *et al*, who developed a promising platform for therapeutics by bioprinting a tumor–stroma model, improving the previously discussed model. In this model, they incorporated triple-negative breast CSCs and stromal cells, by realizing their models with breast-derived bioink. This bioink signed a significant advancement toward 3D *in vitro* models of breast cancer, due to the molecular signatures in the model which ensured a unique profile for embedded breast cancer cells [99].

3D bioprinting has gained tremendous interest in the last years from oncology research [74] due to its ability to combine notions from Materials Engineering with Biology. Bioprinted models can offer promising platforms for novel drugs and therapies testing with a good level of scalability and printability. Starting from 2D cell cultures, 3D *in vitro* models have notably evolved and adapted to the requests of oncology research, by progressively considering the demand for a great TME mimesis, the need to resemble as better as possible the tumor mechanical/biological features, the compartmentalization of the pathology and the scalability of models production (figure 14). Nowadays, hydrogels and moreover 3D bioprinted models seem to offer promising platforms for oncology research, opening the door for personalized medicine and translatability. Lately, the introduction of dECM from breast tissue offers the possibility to decorate bioinks with important molecular sequences typical of the tissues of interest, offering advanced niches where breast cancer cells can exploit their invasive and aggressive behavior [99].

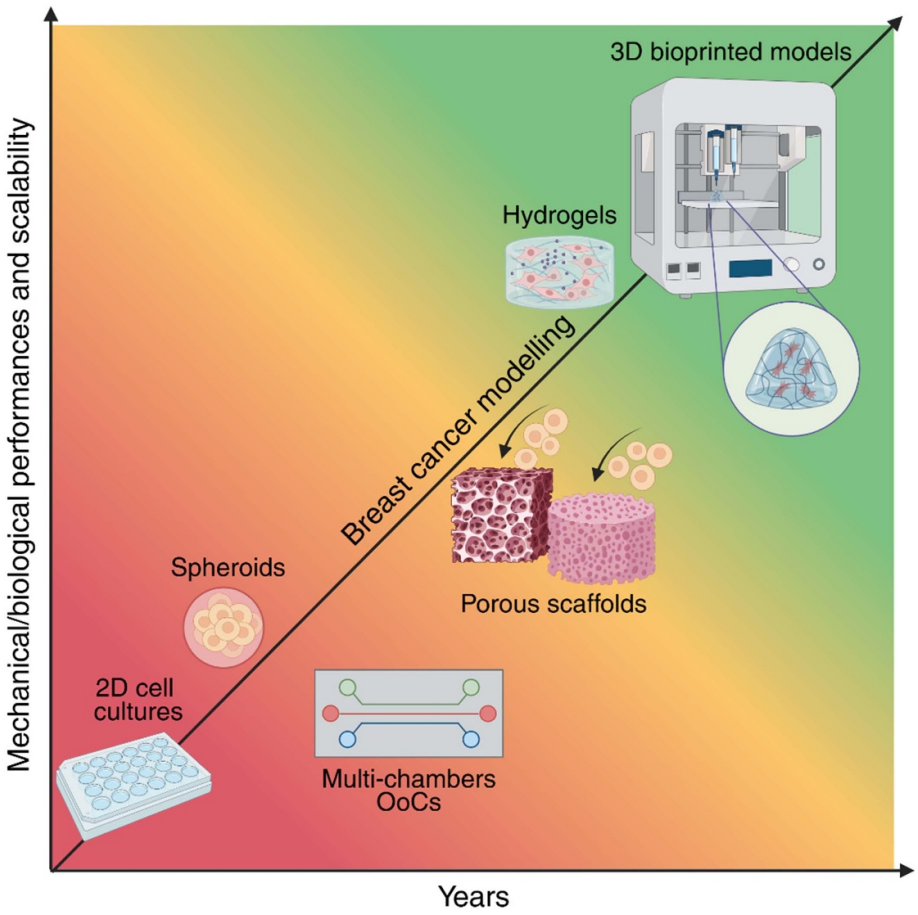

Figure 14. Evolution of engineered 3D constructs for 3D breast cancer modeling. A sustaining matrix with mechanical and biological properties resembling breast cancer was progressively required by oncology research. Scaffolds, hydrogels and bioprinted models furnished a surrounding microenvironment stimulating cells growth, proliferation and communication. 3D bioprinting significantly enhanced the scalability of 3D models production. Created in BioRender. Unipv (2026) https://BioRender.com/4d3vc4g.

3. Discussion

Spheroids, OoCs, and engineered 3D constructs represent promising solutions to elucidate the complex mechanisms of breast tumorigenesis. These models represent a bridge between simplistic 2D cell cultures and living animal models. Although animal models provide a dynamic environment with the presence of an immune system, vasculature, and other naturally occurring features in the physiological TME, they are also time-consuming, laborious, and costly [9]. The use of animal models should be limited, in accordance with the 3R's Principle (*Re*placement, *Re*duction, *Re*finement). Even though achieving the heterogeneity of *in vivo* condition is challenging, developing a model as close as possible to the natural TME could revolutionize oncology research.

We have summarized the advantages and disadvantages of previously discussed 3D *in vitro* models (table 10). Analyzing the applications these models have been intended for, the advantages of engineered 3D constructs for mimicking breast cancer clearly emerge, whereas the limitations of spheroids and OoCs and potential improvements can be discussed. The morphology of spheroids formed by an inner necrotic core and an outer proliferating cell layer, has largely enabled the study of tumor biology and the screening of anticancer drugs. Despite the several advantages of this technology, mainly intended as a significant improvement of 2D cell cultures, some drawbacks persist. For example, difficulties can be faced for large production of spheroids with precise size through standard labware, in handling, maintenance, treatment, and analysis of cellular responses. In addition, limitations also lie in spheroids consistency, control, flexibility, and time-consuming production [16, 44]. Even though spheroids finely match the portion of primary original *in vivo* tumors due to the establishment of oxygen and nutrients gradients, these models lack the possibility of reproducing progressive stages of the pathology [11]. A higher degree of complexity could be reached by considering the inclusion of stromal cells into the spheroid, replicating *in vitro* the interactions between breast cancer cells and healthy cells. Additionally, culturing breast cancer spheroids in an engineered ECM-like material could enhance the possibility to investigate the motility, invasion, and migration capability of metastatic

Table 10. Advantages, disadvantages and requirements of 3D *in vitro* models for breast TME mimicking.

	Advantages	Disadvantages	Requirements
Spheroids	Resembling tumor morphology (*necrotic core + proliferative shell*)	Size-dependent outcomes	Limited possibility for co-cultures Ability in EMT mimicking, but limited outcomes due to the lack of ECM Ease of process and rapid outcomes in drug testing analysis Ability in mimicking tumor hypoxia (internal core), limited angiogenesis
OoCs	Resembling cancer progression and metastasis at the micro-scale	Difficult to handle High fabrication costs Coordination of different technologies	Possibility of co-cultures in compartments, but low complexity degree Mimicry of cell migration towards metastasis-on-chips Ease of process and rapid outcomes in drug testing Ability in re-creating angiogenesis with microchannels, but limited hypoxia mimicry
Engineered 3D constructs	Resembling tumor features with tailorable properties Supporting cells growth and proliferation in 3D ECM	Limited reproducibility Potential cytotoxicity	Possibility of co-cultures with simultaneous assembly of cell-laden biomaterials Ability in re-creating metastasis in portions with different stiffness Possibility to amplify anticancer drugs resistance in screening tests Ability in mimicking hypoxia in portions with different stiffness; improvements in including vasculature-like systems

tumor cells; whereas, integrating spheroids with a perfusion system could overcome the evaporation of culture medium and a continuous re-filling of oxygen, nutrients, and metabolites exchange.

To address critical issues of spheroids, the incorporation of spheroids in OoCs has been proposed. Matching these two technologies for breast cancer modeling has enabled to answer demands from oncology research for a higher degree of complexity and mimesis of TME. Microchannels and microchambers ensured to investigate all those aspects of cancer biology excluded by spheroid nature, e.g. breast cancer cells intravasation and extravasation in peripheral anatomical sites. For instance, OoCs have been considered a huge implementation of spheroid culture, as they responded to the strong request for a compartmentalization of the different tumor anatomical districts. Besides all the previously mentioned advantages, drawbacks still exist with OoCs (table 10). Their complex design can cause possible interferences with drug screening and potential difficulties in providing long-term cultures [16]. Spatial restrictions of microchannels and microchambers inside the devices can restrict the number of biological models which can be simultaneously tested in a single model. Incorporation of microsystems of co-cultures or tri-cultures implies a high degree of handling complexity. Future perspectives could be directed at understanding the mechanisms beyond the role of immune cells and circulating cells in the compartmentalized TME replicated by OoCs [18].

On the other hand, engineered 3D constructs have gained huge insights into Tissue Engineering and Regenerative Medicine to obtain a tunable matrix for breast cancer mimesis. However, there is still an urgent need to increase the availability of tumor biomimetic hydrogels and bioinks to study the crosstalk between the tumor cells and the sustaining matrix [95], which remains largely undiscovered. Limitations can be associated with high costly and bulky instrumentations, for example the printers or crosslinkers [102]; furthermore, the presence of metal ions, photopolymerization initiators, and/or other

crosslinkers may result in a tedious preparation process and undesirable side effects [107].

Nevertheless, among all the investigated approaches for the fabrication of 3D models, engineered 3D constructs currently represent the most promising technology to design and develop 3D *in vitro* models for breast tumor research. Their ability to support cell growth and proliferation within a customizable and physiologically relevant 3D matrix enables a more faithful reproduction of the *in vivo* TME. The features of this sustaining biomaterial can be adjusted, optimized, and monitored over time. Typical cell–cell and cell-ECM interactions can be observed under yet realistic conditions, shortening the gap between *in vitro* models and clinical observations. Moreover, the introduction and evolution of engineered 3D constructs, from scaffolds to bioprinted models, has progressively met the key demands of modern oncology research: scalability, reproducibility, and improved biological mimicry of the breast TME

The major challenges, which oncology research has aimed at in these years of technological improvements, can be summarized as follows:

- resembling the heterogeneity of cell cultures in TME through breast models;
- modeling the metastatic behavior of breast cancer cells;
- recapitulating the *in vivo* drug response and resistance of tumor cells;
- mimicking hypoxia and neo-angiogenesis occurrence *in vitro*.

Stromal cells play a pivotal role in driving breast cancer cells behavior in breast TME. Among non-cancerous cell lines, CAFs and adipocytes have been recognized as the most crucial cells in promoting a malignant phenotype in breast cancer cells. Reciprocal crosstalk between cancer and stromal cells modulates the aggressiveness of breast cancer cells and the altered secretion of adipocytic lipids from adipocytes. In spheroids, the possibility to co-culture pathological and non-malignant cells has been explored through hanging drop and liquid overlay technique, which turned out to be a suitable method for realizing spheroids which incorporate different cell lines [32, 33, 48, 49]. The compartmentalized microarchitecture of OoCs offers a more refined platform if different cell lines are seeded in different microchambers [10, 61, 63, 70]. Nevertheless, this separation between cell lines does not faithfully represent the *in vivo* conditions, where cells are heterogeneously distributed into the TME. Accordingly, engineered 3D constructs emerged as the most promising approach in co-culturing cancerous and non-tumoral cell lines in a unique engineered microenvironment; among these models, bioinks have been widely employed in co-culture due to the possibility to arrange and deposit cells in a controlled manner [52, 95, 101, 102, 106].

Metastasis represents another crucial feature in tumorigenesis, as breast cancer can proliferate and invade the newly formed vasculature colonizing other anatomical districts, such as bone marrow, lungs, and lymph nodes. Metastasis dramatically increases the death rate in patients with a cancer diagnosis. Hence, understanding the signaling pathways driving the metastasis process and how these signals are activated is essential. Spheroids have been extensively used to explore mechanisms associated with breast cancer metastasis, and the alteration of EMT-associated proteins, like E-cadherin [11]. Since the metastasis process can be influenced by the stiffness of the surrounding ECM, the use of spheroids for metastasis investigation is limited due to the absence of a surrounding matrix. To overcome this limitation, embedding spheroid in a natural polymeric material, able to replicate biological cues typical of the natural ECM, as collagen [51], or Matrigel [48], has been proposed. However, spheroids cannot completely resemble the invasiveness capability of breast cancer cells, as their migration depends on several other factors: spheroids size, surrounding ECM, presence of cancer-associated stromal cells, neo-angiogenesis. For these reasons, OoCs have been specifically designed to model the metastatic process. MoCs have been developed as microfluidic devices which incorporate a tumor compartment and a stromal one, with different stiffness, and rigorously compartmentalized [10, 62–64, 69]. Advantage in employing MoCs to study metastasis process resides in the possibility to separate tumor and stromal compartments, and to incorporate an effective vasculature to assess breast cancer cells migration and invasiveness. However, even though the migration of cancer cells can be observed, and the screening of anticancer drugs can be performed, the stiffness-dependence of the surrounding ECM where cancer cells originate and then propagate may not be faithfully resembled.

Engineered 3D constructs address this gap by allowing precise tuning of matrix stiffness and composition. This in turn allows the investigation of the diverse degree of aggressiveness of breast cancer cell lines, strictly depending on the features of the engineered matrix. Cells encapsulated in hydrogels with different features have shown a stiffness-dependent behavior, as observable *in vivo* [92, 96, 97]. In addition, bioprinted models have recently gained a large attention from oncology research due to the possibility to bioprint models that mimic the spatial distribution of cancer mass, contributing to study their aggressiveness and metastatic behavior: an inner core of breast cancer surrounded by stromal non-cancerous cells [95, 101].

Even though engineered 3D constructs stand up as promising technology for metastasis mimicry, these models today lack an effective system of

nutrients/oxygen/metabolites exchange, which prevents cells from migrating from a tumoral compartment to a non-malignant one. Improvements under development include an efficient vasculature-like system into scaffold-based, hydrogel-based and bioprinted models, enhancing their degree of complexity and cells viability. Future perspectives are now directed to enrich engineered 3D constructs with systems of dynamic perfusion, to ensure the mimesis of the vasculature and lymphatic systems.

Drug response from malignant cells is deeply affected by the surrounding environment in 3D *in vitro* models compared to monolayer cultures. Due to their easy process of obtainment, spheroids have been extensively investigated for testing drugs and breast cancer cells response [37, 43–45]. However, spheroid responses vary significantly depending on the drug concentration, on the spheroid size, and on the cells type. Alternatively, DDSs have also been implemented to obtain a more similar response to the *in vivo* condition, compared to the free diffusion of drugs into the spheroids [46, 47]. For the possibility to embed efficient microchannels, OoCs have been fabricated for testing anticancer drugs [57, 64, 65, 70]. While spheroids and OoCs offer high-throughput and rapid screening, engineered 3D constructs can provide a more physiologically relevant platform. Breast cancer cells in these 3D models show a higher drug resistance since they are *seeded onto* or *embedded into* a construct which resembles biological cues typical of breast tumor matrix better than in spheroids or OoCs. Rapid production of bioprinted models also ensures a huge improvement in the scalability of the approach, successfully responding to a strong request from oncology research. For instance, engineered constructs nowadays represent the most promising alternative to investigate new anticancer treatments and consequently obtain the most faithfully resistance response from breast cancer cells compared to the *in vivo* condition [73, 82, 85, 87].

Tumorigenesis critically alters breast TME features, inducing a condition of hypoxia, which stresses cells to promote new vasculature. Breast cancer cells force these newly formed fenestrations to migrate from the original tumor site to other anatomical districts. The complex TME generally drives all these features, which are all connected towards complex molecular and cellular pathways. Among 3D models, spheroids easily replicate this condition of hypoxia due to their assembling in an inner necrotic core and an outer proliferating cell layer. However, the dependence on spheroid size still represents a huge limitation on the involvement of these models for breast cancer hypoxia mimicking. Contrarily, OoCs can incorporate microchannels to simulate the tumor vasculature [10, 58, 66–68], assessing the capability of breast cancer cells to intravasate into the microchannels and extravasate in non-malignant compartments. However, replicating hypoxia is challenging in OoCs. Engineered 3D constructs are nowadays investigated to mimic hypoxia conditions by tailoring the stiffness of the surrounding ECM, which can be increased by coupling different biomaterials or by increasing crosslinking compounds concentration; contrarily, vascularization remains challenging and under investigation. Among these models, bioprinted models can achieve a better inner necrotic core and proliferative outer layer mimicry by spatially arranging bioink deposition in a well-defined and controlled manner.

Although great improvements have been achieved in time in generating 3D *in vitro* breast tumor models, the existing models still have unsolved challenges and limitations. One problem generally related to 3D *in vitro* models can be the lack of culture medium suitable for all the cell lines when co-cultured together into the same model. This limitation could be solved by incorporating necessary growth factors, cytokines and metalloproteinases (MMPs) into the stromal and tumor compartments, or by enriching the models with sustainment factors. Additionally, future perspective will be focused on the incorporation of macrophages or regulatory immune cells into the models, which control the reaction of endothelial cells or pericytes, which are responsible for angiogenesis. Vascularization is still an open challenge in biofabrication, as diverse promising approaches have been implemented to obtain vascularized models. Recently, modern approaches of dynamic culture are arising to furnish a continuous perfusion of the hydrogels or bioprinted models in a confined system, which ensure the cells to grow under physiological-like shear stresses.

Among the investigated approaches, a particular fabrication technique could be considered more promising than others in a specific issue but could show limitations by considering a different application (table 11). To address this gap, future perspectives could be also directed on the combination of two or more approaches to generate promising 3D *in vitro* models which could answer the requirements of the oncology research.

The progressive improvements discussed in this review have narrowed the gap between *in vivo* physiology and *in vitro* experimentation, marking a decisive step forward in the development of relevant 3D breast tumor models to facilitate drug research and clinical tests and accelerate the translatability of patient-specific solutions. Among the different approaches explored, hydrogel-based and bioprinted models are currently arising as the most promising methods for 3D *in vitro* modeling of breast cancer. Their tunable physicochemical properties, and ability to mimic the ECM provide an ideal microenvironment for realistic tumor simulation. These systems represent a natural evolution from traditional 2D monolayers, multicellular spheroids, and OoCs technologies, integrating the strengths of each while overcoming their inherent limitations. By enabling

Table 11. Classification of the best techniques based on the main focus of the research.

Research focus	Best techniques	Explanation
Tumor invasion & migration	OoCs Hydrogels 3D bioprinting	OoCs allow migration of different cell species through the connecting microchannels Hydrogels allow invasion into soft matrices 3D bioprinting allows simultaneous bioprinting of different *anatomical* compartments
Drug penetration & resistance	Spheroids OoCs	Spheroids mimic diffusion barriers Chips enable dynamic drug perfusion
Vascularization	OoCs 3D bioprinting	Chips can integrate perfusable microvessels Bioprinting allows predefined patterning of endothelial networks
Mechanotransduction/ECM Stiffness Effects	Scaffolds Hydrogels 3D bioprinting	Scaffolds best for controlled mechanical properties Hydrogels and bioprinting for tunable viscoelasticity to best fit mechanical features and represent the different stages in tumorigenesis
High-throughput drug screening	Spheroids Hydrogels 3D bioprinting	These approaches are simple, cost-effective, and scalable; ideal for pharmaceutical screening pipelines

precise spatial organization, scalable fabrication, and dynamic control over biological and mechanical cues, hydrogel-based and bioprinted models now fulfill key requirements of modern oncology research: reproducibility, scalability, and physiological complexity. As such, they constitute a cornerstone in the transition toward next-generation preclinical platforms

4. Conclusions

Promising solutions for 3D *in vitro* breast cancer models have been developed and investigated in literature. Starting from simplistic 2D cell cultures, technologies have evolved, and the degree of complexity has gradually increased during the last years, improving the mimicry of the complex mechanisms behind cell–cell and cell-TME interactions as required from oncology research. Nowadays, hydrogels and bioprinted models are considered the most promising technologies for 3D breast cancer models fabrication, due to the possibility of sustaining and embedding cells within an engineered 3D matrix, which is scalable, adjustable, tunable, and at the same time can faithfully resemble the features of the *in vivo* TME.

Data availability statement

The data that support the findings of this study are available upon reasonable request from the authors.

Author contributions

M Pitton 0009-0009-7817-0310
Conceptualization (equal), Formal analysis (equal), Writing – original draft (equal)

L Draghi 0000-0003-4744-7777
Supervision (equal), Writing – review & editing (equal)

S Farè 0000-0002-0303-1131
Supervision (equal), Writing – review & editing (equal)

References

[1] Newman L 2023 Oncologic anthropology: global variations in breast cancer risk, biology, and outcome *J. Surg. Oncol.* **128** 959–66
[2] Bray F, Laversanne M, Sung H, Ferlay J, Siegel R L, Soerjomataram I and Jemal A 2024 Global cancer statistics 2022: GLOBOCAN estimates of incidence and mortality worldwide for 36 cancers in 185 countries *CA Cancer J. Clin.* **74** 229–63
[3] Li J, Fang K, Choppavarapu L, Yang K, Yang Y, Wang J, Cao R, Jatoi I and Jin V X 2021 Hi-C profiling of cancer spheroids identifies 3D-growth-specific chromatin interactions in breast cancer endocrine resistance *Clin. Clin. Epigenet* **13** 175
[4] Nair L, Mukherjee S, Kaur K, Murphy C M, Ravichandiran V, Roy S and Singh M 2023 Multi compartmental 3D breast cancer disease model–recapitulating tumor complexity in in-vitro *Biochim. Biophys. Acta* **1867** 130361
[5] Zhang W, Li C, Baguley B C, Zhou F, Zhou W, Shaw J P, Wang Z, Wu Z and Liu J 2016 Optimization of the formation of embedded multicellular spheroids of MCF-7 cells: how to reliably produce a biomimetic 3D model *Anal. Biochem.* **515** 47–54
[6] Caffa I *et al* 2020 Fasting-mimicking diet and hormone therapy induce breast cancer regression *Nature* **583** 620–4
[7] Parhi L *et al* 2020 Breast cancer colonization by fusobacterium nucleatum accelerates tumor growth and metastatic progression *Nat. Commun.* **11** 3259
[8] Regua A T, Arrigo A, Doheny D, Wong G L and Lo H-W 2021 Transgenic mouse models of breast cancer *Cancer Lett.* **516** 73–83

[9] Bahcecioglu G, Basara G, Ellis B W, Ren X and Zorlutuna P 2020 Breast cancer models: engineering the tumor microenvironment *Acta Biomater.* **106** 1–21
[10] Chi C, Lao Y-H, Ahmed A H R, Benoy E C, Li C, Dereli-Korkut Z, Fu B M, Leong K W and Wang S 2020 High-throughput tumor-on-a-chip platform to study tumor–stroma interactions and drug pharmacokinetics *Adv. Healthcare Mater.* **9** 2000880
[11] Huang Z, Yu P and Tang J 2020 characterization of triple-negative breast cancer MDA-MB-231 cell spheroid model *Oncol. Targets Ther.* **13** 5395–405
[12] Kundu M, Butti R, Panda V K, Malhotra D, Das S, Mitra T, Kapse P, Gosavi S W and Kundu G C 2024 Modulation of the tumor microenvironment and mechanism of immunotherapy-based drug resistance in breast cancer *Mol. Cancer* **23** 92
[13] Zhang W, Lee A, Tiwari A K and Yang M Q 2024 Characterizing the tumor microenvironment and its prognostic impact in breast cancer *Cells* **13** 1518
[14] Danenberg E *et al* 2022 Breast tumor microenvironment structures are associated with genomic features and clinical outcome *Nat. Genet.* **54** 660–9
[15] Banerjee M and Rajeswari V D 2023 A novel cross-communication of HIF-1α and HIF-2α with Wnt signaling in TNBC and influence of hypoxic microenvironment in the formation of an organ-on-chip model of breast cancer *Med. Oncol.* **40** 245
[16] Huerta-Reyes M and Aguilar-Rojas A 2021 Three-dimensional models to study breast cancer (Review) *Int. J. Oncol.* **58** 331–43
[17] Mukherjee A, Bilecz A J and Lengyel E 2022 The adipocyte microenvironment and cancer *Cancer Metastasis Rev.* **41** 575–87
[18] Kalot R, Mhanna R and Talhouk R 2022 Organ-on-a-chip platforms as novel advancements for studying heterogeneity, metastasis, and drug efficacy in breast cancer *Pharmacol. Ther.* **237** 108156
[19] Liang Y, Zhang H, Song X and Yang Q 2020 Metastatic heterogeneity of breast cancer: molecular mechanism and potential therapeutic targets *Semin. Cancer Biol.* **60** 14–27
[20] Liu C, Li M, Dong Z-X, Jiang D, Li X, Lin S, Chen D, Zou X, Zhang X-D and Luker G D 2021 Heterogeneous microenvironmental stiffness regulates pro-metastatic functions of breast cancer cells *Acta Biomater.* **131** 326–40
[21] Shah L, Latif A, Williams K J and Tirella A 2022 Role of stiffness and physico-chemical properties of tumour microenvironment on breast cancer cell stemness *Acta Biomater.* **152** 273–89
[22] Swaminathan S, Hamid Q, Sun W and Clyne A M 2019 Bioprinting of 3D breast epithelial spheroids for human cancer models *Biofabrication* **11** 025003
[23] Zhao L, Xiu J, Liu Y, Zhang T, Pan W, Zheng X and Zhang X 2019 A 3D printed hanging drop dripper for tumor spheroids analysis without recovery *Sci. Rep.* **9** 19717
[24] Cheng G J, Leung E Y and Singleton D C 2022 In vitro breast cancer models for studying mechanisms of resistance to endocrine therapy *Explor. Target. Anti.* **3** 297–320
[25] Ravichandran A, Clegg J, Adams M N, Hampson M, Fielding A and Bray L J 2021 3D breast tumor models for radiobiology applications *Cancers* **13** 5714
[26] Boix-Montesinos P, Soriano-Teruel P M, Armiñán A, Orzáez M and Vicent M J 2021 The past, present, and future of breast cancer models for nanomedicine development *Adv. Drug Deliv. Rev.* **173** 306–30
[27] Katti K S, Jasuja H, Kar S and Katti D R 2021 Nanostructured biomaterials for in vitro models of bone metastasis cancer *Curr. Opin. Biomed. Eng.* **17** 100254
[28] Sitarski A M, Fairfield H, Falank C and Reagan M R 2018 3D tissue engineered in vitro models of cancer in bone *ACS Biomater. Sci. Eng.* **4** 324–36
[29] González Díaz E C, Sinha S, Avedian R S and Yang F 2019 Tissue-engineered 3D models for elucidating primary and metastatic bone cancer progression *Acta Biomater.* **99** 18–32
[30] Brock E J, Ji K, Shah S, Mattingly R R and Sloane B F 2019 In vitro models for studying invasive transitions of ductal carcinoma in situ *J. Mammary Gland Biol. Neoplasia* **24** 1–15
[31] Cleversey C, Robinson M and Willerth S M 2019 3D printing breast tissue models: a review of past work and directions for future work *Micromachines* **10** 501
[32] Domingues M, Leite Pereira C, Sarmento B and Castro F 2023 Mimicking 3D breast tumor-stromal interactions to screen novel cancer therapeutics *Eur. J. Pharm Sci.* **190** 106560
[33] Ferreira L P, Gaspar V M, Monteiro M V, Freitas B, Silva N J O and Mano J F 2021 Screening of dual chemo-photothermal cellular nanotherapies in organotypic breast cancer 3D spheroids *J. Control. Release* **331** 85–102
[34] Hong S and Song J M 2022 3D bioprinted drug-resistant breast cancer spheroids for quantitative in situ evaluation of drug resistance *Acta Biomater.* **138** 228–39
[35] Thakuri P S, Ham S L, Luker G D and Tavana H 2016 Multiparametric analysis of oncology drug screening with aqueous two-phase tumor spheroids *Mol. Pharm.* **13** 3724–35
[36] Kingsley D M, Roberge C L, Rudkouskaya A, Faulkner D E, Barroso M, Intes X and Corr D T 2019 Laser-based 3D bioprinting for spatial and size control of tumor spheroids and embryoid bodies *Acta Biomater.* **95** 357–70
[37] Mukundan S, Bell J, Teryek M, Hernandez C, Love A C, Parekkadan B and Chan L L-Y 2022 Automated assessment of cancer drug efficacy on breast tumor spheroids in Aggrewell™400 plates using image cytometry *J. Fluoresc.* **32** 521–31
[38] Ong C S, Yesantharao P, Huang C Y, Mattson G, Boktor J, Fukunishi T, Zhang H and Hibino N 2018 3D bioprinting using stem cells *Pediatr. Res.* **83** 223–31
[39] Hong S and Song J M 2023 High-resolution in situ high-content imaging of 3D-bioprinted single breast cancer spheroids for advanced quantification of Benzo(*a*)pyrene carcinogen-induced breast cancer stem cells *ACS Appl. Mater. Interfaces* **15** 11416–30
[40] Ham S L, Joshi R, Luker G D and Tavana H 2016 Engineered breast cancer cell spheroids reproduce biologic properties of solid tumors *Adv. Healthcare Mater.* **5** 2788–98
[41] Froehlich K *et al* 2016 Generation of multicellular breast cancer tumor spheroids: comparison of different protocols *J. Mammary Gland Biol. Neoplasia* **21** 89–98
[42] Eckhardt B L *et al* 2018 Clinically relevant inflammatory breast cancer patient-derived xenograft–derived ex vivo model for evaluation of tumor-specific therapies *PLoS One* **13** e0195932
[43] Chen G, Liu W and Yan B 2022 Breast cancer MCF-7 cell spheroid culture for drug discovery and development *J. Cancer Ther.* **13** 117–30
[44] Seeto W J, Tian Y, Pradhan S, Minond D and Lipke E A 2022 Droplet microfluidics-based fabrication of monodisperse poly(ethylene glycol)-fibrinogen breast cancer microspheres for automated drug screening applications *ACS Biomater. Sci. Eng.* **8** 3831–41
[45] Balsa L M, Rodriguez M R, Parajón-Costa B S, González-Baró A C, Lavecchia M J and León I E 2022 Anticancer activity and mechanism of action evaluation of an acylhydrazone Cu(II) complex toward breast cancer cells, spheroids, and mammospheres *ChemMedChem* **17** e202100520
[46] Schneible J D, Young A T, Daniele M A and Menegatti S 2020 Chitosan hydrogels for synergistic delivery of chemotherapeutics to triple negative breast cancer cells and spheroids *Pharma Res.* **37** 142
[47] Granja A, Lima-Sousa R, Alves C G, de Melo-diogo D, Pinheiro M, Sousa C T, Correia I J and Reis S 2021 Mitoxantrone-loaded lipid nanoparticles for breast cancer

therapy—quality-by-design approach and efficacy assessment in 2D and 3D in vitro cancer models *Int. J. Pharm.* **607** 121044
[48] Li A, Muenst S, Hoffman J, Starck L, Sarem M, Fischer A, Hutter G and Shastri V P 2022 Mesenchymal-endothelial nexus in breast cancer spheroids induces vasculogenesis and local invasion in a CAM model *Commun. Biol.* **5** 1303
[49] Paré M *et al* 2020 Breast cancer mammospheres secrete Adrenomedullin to induce lipolysis and browning of adjacent adipocytes *BMC Cancer* **20** 784
[50] Horder H *et al* 2021 Bioprinting and differentiation of adipose-derived stromal cell spheroids for a 3D breast cancer-adipose tissue model *Cells* **10** 803
[51] Perrin L, Belova E, Bayarmagnai B, Tüzel E and Gligorijevic B 2022 Invadopodia enable cooperative invasion and metastasis of breast cancer cells *Commun. Biol.* **5** 758
[52] Boroojeni F R, Naeimipour S, Lifwergren P, Abrahamsson A, Dabrosin C, Selegård R and Aili D 2024 Proteolytic remodeling of 3D bioprinted tumor microenvironments *Biofabrication* **16** 025002
[53] Horder H *et al* 2024 Cancer cell migration depends on adjacent ASC and adipose spheroids in a 3D bioprinted breast cancer model *Biofabrication* **16** 035031
[54] Marconi G D, Porcheri C, Trubiani O and Mitsiadis T A 2021 Three-dimensional culture systems for dissecting notch signalling in health and disease *Int. J. Mol. Sci.* **22** 12473
[55] Bein A, Shin W, Jalili-Firoozinezhad S, Park M H, Sontheimer-Phelps A, Tovaglieri A, Chalkiadaki A, Kim H J and Ingber D E 2018 Microfluidic organ-on-a-chip models of human intestine *Cell Mol. Gastroenterol. Hepatol.* **5** 659–68
[56] Tajeddin A and Mustafaoglu N 2021 Design and fabrication of organ-on-chips: promises and challenges *Micromachines* **12** 1443
[57] Flont M, Dybko A and Jastrzębska E 2023 A layered cancer-on-a-chip system for anticancer drug screening and disease modeling *Analyst* **148** 5486–95
[58] Lee G, Kim S J and Park J-K 2023 Fabrication of a self-assembled and vascularized tumor array via bioprinting on a microfluidic chip *Lab Chip* **23** 4079–91
[59] Frankman Z D, Jiang L, Schroeder J A and Zohar Y 2022 Application of microfluidic systems for breast cancer research *Micromachines* **13** 152
[60] Jouybar M, Sleeboom J J F, Vaezzadeh E, Sahlgren C M and Den Toonder J M J 2023 An in vitro model of cancer invasion with heterogeneous ECM created with droplet microfluidics *Front. Bioeng. Biotechnol.* **11** 1267021
[61] Lam S F, Bishop K W, Mintz R, Fang L and Achilefu S 2021 Calcium carbonate nanoparticles stimulate cancer cell reprogramming to suppress tumor growth and invasion in an organ-on-a-chip system *Sci. Rep.* **11** 9246
[62] Lugo-Cintrón K M, Ayuso J M, White B R, Harari P M, Ponik S M, Beebe D J, Gong M M and Virumbrales-Muñoz M 2020 Matrix density drives 3D organotypic lymphatic vessel activation in a microfluidic model of the breast tumor microenvironment *Lab Chip* **20** 1586–600
[63] Conceição F, Sousa D M, Loessberg-Zahl J, Vollertsen A R, Neto E, Søe K, Paredes J, Leferink A and Lamghari M 2022 A metastasis-on-a-chip approach to explore the sympathetic modulation of breast cancer bone metastasis *Mater. Today Bio* **13** 100219
[64] Ozer L Y, Fayed H S, Ericsson J and Haj Zen A A 2024 Development of a cancer metastasis-on-chip assay for high throughput drug screening *Front. Oncol.* **13** 1269376
[65] Prince E *et al* 2022 Microfluidic arrays of breast tumor spheroids for drug screening and personalized cancer therapies *Adv. Healthcare Mater.* **11** 2101085
[66] Nashimoto Y, Okada R, Hanada S, Arima Y, Nishiyama K, Miura T and Yokokawa R 2020 Vascularized cancer on a chip: the effect of perfusion on growth and drug delivery of tumor spheroid *Biomaterials* **229** 119547
[67] Su C, Chuah Y J, Ong H B, Tay H M, Dalan R and Hou H W 2021 A facile and scalable hydrogel patterning method for microfluidic 3D cell culture and spheroid-in-gel culture array *Biosensors* **11** 509
[68] Kwak T J and Lee E 2020 In vitro modeling of solid tumor interactions with perfused blood vessels *Sci. Rep.* **10** 20142
[69] Aung A, Kumar V, Theprungsirikul J, Davey S K and Varghese S 2020 An engineered tumor-on-a-chip device with breast cancer–immune cell interactions for assessing T-cell recruitment *Cancer Res.* **80** 263–75
[70] Flont M and Jastrzębska E 2023 A multi-layer breast cancer model to study the synergistic effect of photochemotherapy *Micromachines* **14** 1806
[71] Verbruggen S W, Nolan J, Duffy M P, Pearce O M T, Jacobs C R and Knight M M 2024 A novel primary cilium-mediated mechanism through which osteocytes regulate metastatic behavior of both breast and prostate cancer cells *Adv. Sci.* **11** 2305842
[72] Teixeira A M and Martins P 2023 A review of bioengineering techniques applied to breast tissue: mechanical properties, tissue engineering and finite element analysis *Front. Bioeng. Biotechnol.* **11** 1161815
[73] Xu J, Yang S, Su Y, Hu X, Xi Y, Cheng Y Y, Kang Y, Nie Y, Pan B and Song K 2022 A 3D bioprinted tumor model fabricated with gelatin/sodium alginate/decellularized extracellular matrix bioink *Int. J. Bioprinting* **9** 630
[74] Sbrana F V *et al* 2021 3D bioprinting allows the establishment of long-term 3D culture model for chronic lymphocytic leukemia cells *Front. Immunol.* **12** 639572
[75] Redmond J, McCarthy H, Buchanan P, Levingstone T J and Dunne N J 2021 Advances in biofabrication techniques for collagen-based 3D in vitro culture models for breast cancer research *Mater. Sci. Eng. C* **122** 111944
[76] Chinnasami H, Dey M K and Devireddy R 2023 Three-dimensional scaffolds for bone tissue engineering *Bioengineering* **10** 759
[77] Xydeas T, Siegmann K, Sinkus R, Krainick-Strobel U, Miller S and Claussen C D 2005 Magnetic resonance elastography of the breast: correlation of signal intensity data with viscoelastic properties *Invest. Radiol.* **40** 412–20
[78] McKnight A L, Kugel J L, Rossman P J, Manduca A, Hartmann L C and Ehman R L 2002 MR elastography of breast cancer: preliminary results *Am. J. Roentgenol.* **178** 1411–7
[79] Srivastava A, Verma Y, Rao K D and Gupta P K 2011 Determination of elastic properties of resected human breast tissue samples using optical coherence tomographic elastography *Strain* **47** 75–87
[80] Samani A, Zubovits J and Plewes D 2007 Elastic moduli of normal and pathological human breast tissues: an inversion-technique-based investigation of 169 samples *Phys. Med. Biol.* **52** 1565–76
[81] Umemoto T, Ueno E, Matsumura T, Yamakawa M, Bando H, Mitake T and Shiina T 2014 Ex vivo and *in vivo* assessment of the non-linearity of elasticity properties of breast tissues for quantitative strain elastography *Ultrasound Med. Biol.* **40** 1755–68
[82] Lv K, Zhu J, Zheng S, Jiao Z, Nie Y, Song F, Liu T and Song K 2021 Evaluation of inhibitory effects of geniposide on a tumor model of human breast cancer based on 3D printed Cs/gel hybrid scaffold *Mater. Sci. Eng. C* **119** 111509
[83] Rezaeeyazdi M, Colombani T, Eggermont L J and Bencherif S A 2022 Engineering hyaluronic acid-based cryogels for CD44-mediated breast tumor reconstruction *Mater. Today Bio* **13** 100207
[84] Tomar A, Uysal-Onganer P, Basnett P, Pati U and Roy I 2022 3D disease modelling of hard and soft cancer using PHA-based scaffolds *Cancers* **14** 3549
[85] Su Y, Hu X, Kang Y, Zhang C, Cheng Y Y, Jiao Z, Nie Y and Song K 2023 Curcumin nanoparticles combined with 3D

printed bionic tumor models for breast cancer treatment *Biofabrication* **15** 014105
[86] Redmond J, McCarthy H O, Buchanan P, Levingstone T J and Dunne N J 2022 Development and characterisation of 3D collagen-gelatin based scaffolds for breast cancer research *Biomater. Adv.* **142** 213157
[87] Rosendahl J *et al* 2021 3D printed nanocellulose scaffolds as a cancer cell culture model system *Bioengineering* **8** 97
[88] Svanström A *et al* 2021 Optimized alginate-based 3D printed scaffolds as a model of patient derived breast cancer microenvironments in drug discovery *Biomed. Mater.* **16** 045046
[89] Hipwood L, Clegg J, Weekes A, Davern J W, Dargaville T R, Meinert C and Bock N 2022 Semi-synthetic click-gelatin hydrogels as tunable platforms for 3D cancer cell culture *Gels* **8** 821
[90] Shi Y, Wang Z, Zhou X, Lin C, Chen C, Gao B, Xu W, Zheng X, Wu T and Wang H 2023 Preparation of a 3D printable high-performance GelMA hydrogel loading with magnetic cobalt ferrite nanoparticles *Front. Bioeng. Biotechnol.* **11** 1132192
[91] Nasser M and Ghosh G 2022 Engineering tumor constructs to study matrix-dependent angiogenic signaling of breast cancer cells *Biotechnol. Prog.* **38** e3250
[92] Shah L, Latif A, Williams K J, Mancuso E and Tirella A 2023 Invasion and secondary site colonization as a function of in vitro primary tumor matrix stiffness: breast to bone metastasis *Adv. Healthcare Mater.* **12** 2201898
[93] De Dios-Figueroa G T, Aguilera-Márquez J D R, García-Uriostegui L, Hernández-Gutiérrez R, Camacho-Villegas T A and Lugo-Fabres P H 2023 Embedded living HER2+ cells in a 3D gelatin–alginate hydrogel as an in vitro model for immunotherapy delivery for breast cancer *Polymers* **15** 3726
[94] Barros Da Silva P, Oliveira R J A, Araújo M, Caires H R, Bidarra S J and Barrias C C 2024 An integrative alginate-based 3D in vitro model to explore epithelial-stromal cell dynamics in the breast tumor microenvironment *Carbohydr. Polym.* **342** 122363
[95] Blanco-Fernandez B, Ibañez-Fonseca A, Orbanic D, Ximenes-Carballo C, Perez-Amodio S, Rodríguez-Cabello J C and Engel E 2023 Elastin-like recombinamer hydrogels as platforms for breast cancer modeling *Biomacromolecules* **24** 4408–18
[96] Clough H C, O'Brien M, Zhu X, Miller A F, Saiani A and Tsigkou O 2021 Neutrally charged self-assembling peptide hydrogel recapitulates in vitro mechanisms of breast cancer progression *Mater. Sci. Eng. C* **127** 112200
[97] Chia J Y, Miki T, Mihara H and Tsutsumi H 2021 Biofunctional supramolecular hydrogels fabricated from a short self-assembling peptide modified with bioactive sequences for the 3D culture of breast cancer MCF-7 cells *Bioorg. Med. Chem.* **46** 116345
[98] Lingard E *et al* 2024 Optimising a self-assembling peptide hydrogel as a Matrigel alternative for 3-dimensional mammary epithelial cell culture *Biomater. Adv.* **160** 213847
[99] González-Callejo P, García-Astrain C, Herrero-Ruiz A, Henriksen-Lacey M, Seras-Franzoso J, Abasolo I and Liz-Marzán L M 2024 3D bioprinted tumor-stroma models of triple-negative breast cancer stem cells for preclinical targeted therapy evaluation *ACS Appl. Mater. Interfaces* **16** 27151–63
[100] Davern J W, Hipwood L, Bray L J, Meinert C and Klein T J 2024 Addition of Laponite to gelatin methacryloyl bioinks improves the rheological properties and printability to create mechanically tailorable cell culture matrices *APL Bioeng.* **8** 016101
[101] González-Callejo P, Vázquez-Aristizabal P, García-Astrain C, Jimenez de Aberasturi D, Henriksen-Lacey M, Izeta A and Liz-Marzán L M 2023 3D bioprinted breast tumor-stroma models for pre-clinical drug testing *Mater. Today Bio* **23** 100826
[102] Chaji S, Al-Saleh J and Gomillion C 2020 Bioprinted three-dimensional cell-laden hydrogels to evaluate adipocyte-breast cancer cell interactions *Gels* **6** 10
[103] Dankó T *et al* 2022 Characterisation of 3D bioprinted human breast cancer model for in vitro drug and metabolic targeting *Int. J. Mol. Sci.* **23** 7444
[104] Schmid R *et al* 2020 Comparison of hydrogels for the development of well-defined 3D cancer models of breast cancer and melanoma *Cancers* **12** 2320
[105] Blanco-Fernandez B, Rey-Vinolas S, Bağcı G, Rubi-Sans G, Otero J, Navajas D, Perez-Amodio S and Engel E 2022 Bioprinting decellularized breast tissue for the development of three-dimensional breast cancer models *ACS Appl. Mater. Interfaces* **14** 29467–82
[106] Shi W *et al* 2023 Embedded bioprinting of breast tumor cells and organoids using low-concentration collagen-based bioinks *Adv. Healthcare Mater.* **12** 2300905
[107] Zhang Y, Chen H and Li J 2022 Recent advances on gelatin methacrylate hydrogels with controlled microstructures for tissue engineering *Int. J. Biol. Macromol.* **221** 91–107